applied sciences

MDPI

Article

The Quality of *Scutellaria baicalensis* Georgi Is Effectively Affected by Lithology and Soil's Rare Earth Elements (REEs) Concentration

Zijian Sun [1,2], Wei Shen [1], Weixuan Fang [3,*], Huiqiong Zhang [2], Ziran Chen [2], Lianghui Xiong [2] and Tianhao An [2]

[1] School of Earth Sciences and Resources, China University of Geosciences (Beijing), Beijing 100083, China
[2] Beijing Institute of Geology for Mineral Resources Co., Ltd., Beijing 100012, China
[3] China Non-Ferrous Metals Resource Geological Survey, Beijing 100012, China
* Correspondence: weixuanfang123@163.com

Abstract: The top-geoherb "Rehe *Scutellaria baicalensis*" was naturally distributed on Yanshan Mountain in Chengde city, Hebei Province, China. Exploring the influences of parent materials on the quality of the top-geoherbs in terms of micronutrient elements is of great significance for the protection of origin and for optimizing replanting patterns of *Scutellaria baicalensis*. In this study, three habitats of *Scutellaria baicalensis* with contrasting geopedological conditions, i.e., naturally grown habitats (NGHs), artificial planting habitats (APHs), and biomimetic cultivation habitats (BCHs), are taken as objects to probe the influences of parent materials on the quality of *Scutellaria baicalensis* in terms of rare earth elements (REEs) by testing on REEs concentrations in the weathering profiles, rhizosphere soil and growing *Scutellaria baicalensis*, as well as their flavonoid compound contents. Hornblende-gneiss was the parent rock in NGHs, whose protolith was femic volcanic rock. Loess was the parent rock in APHs and BCHs. REEs were more abundant in hornblende-gneiss than loess, and therefore, soils developed in NGHs contained higher REE concentrations than those in APHs, which was lower than BCHs after REE-rich micro-fertilizers application. The coefficient of variation (CV) of REEs concentrations in the rhizosphere soils of hornblende-gneiss was higher than that in loess. It possibly was attributed to the complicated minerals compositions and various minerals' grain sizes of hornblende-gneiss, resulting in the variety of weathering intensity involving eluviation, leaching, adsorption, etc., as well as weathering productions, dominated by clay minerals and Fe-(hydro)oxide, and ultimately the remarkable differences in the migrations, enrichments and fractionations within REEs. The biological absorption coefficients (BACs) of REEs for *Scutellaria baicalensis* decreased in the order of NGHs > APHs > BCHs. Roots of *Scutellaria baicalensis* contained similar ΣREE in NGHs (2.02 mg·kg^{-1}) and BCHs (2.04 mg·kg^{-1}), which were higher than that in APHs (1.78 mg·kg^{-1}). Soils developed in hornblende-gneiss were characterized by lower clay fraction content and overall alkalinity with a pH value of 8.06. The absorption and utilization efficiency of REEs for *Scutellaria baicalensis* in NGHs was higher than in APHs and BCHs. Flavonoid compounds, effective constituents of *Scutelleria baicalensis*, showed more accumulations in NGHs than APHs and BCHs, implying their optimal quality of *Scutellaria baicalensis* in NGHs. Flavonoid compounds were remarkably correlated with REEs in the roots, suggesting the influence of REEs concentrations on the quality of *Scutellaria baicalensis*. It can be concluded that high REEs and micronutrient element concentrations of hornblende-gneiss favored the synthesis and accumulation of flavonoid compounds in *Scutellaria baicalensis* after the activation of endocytosis induced by REEs.

Keywords: parent materials; weathering; geoherbs; gneiss; flavonoid compounds

Citation: Sun, Z.; Shen, W.; Fang, W.; Zhang, H.; Chen, Z.; Xiong, L.; An, T. The Quality of *Scutellaria baicalensis* Georgi Is Effectively Affected by Lithology and Soil's Rare Earth Elements (REEs) Concentration. *Appl. Sci.* **2023**, *13*, 3086. https://doi.org/10.3390/app13053086

Academic Editor: José A. González-Pérez

Received: 9 December 2022
Revised: 21 January 2023
Accepted: 1 February 2023
Published: 27 February 2023

1. Introduction

Geoherb is a term used by ancient Chinese to describe the inter-species variation of Chinese medicines relevant to the geographical variation, and top-geoherb (Dao-di Herbs) is the population of a geoherb growing in habitats with natural conditions and ecological

environment, featuring proverbial superior qualities, better curative effect and popularly used in traditional Chinese medicine clinical practice [1–3], such as *Lycium barbarum* L. from Ningxia, *Radix Angelicae* from Hangzhou, *Radix Rehmanniae* from Henan and *Scutellaria baicalensis* from Rehe in China [4]. Biological factors, e.g., species and intrinsic nature, and geo-environmental factors, e.g., physical and chemical characteristics of parent rock and weathering productions, jointly exert a crucial control on the formation of top-geoherbs' traits. As one of the critical material bases of traditional Chinese medicines, micronutrient elements significantly regulated and controlled the activity of many biological molecules (proteins, enzymes, and hormones) by taking part in enzymatic structures, constructing electron transport systems as carriers, and participating in the synthesis of hormones and vitamins, which ultimately influenced the metabolic activities and accumulation of effective constituents in medicines [5,6]. Therefore, micronutrient element assemblages played a decisive role in forming top-geoherbs' traits [5–8].

Rare earth elements (REEs) are a group of chemically similar elements behaving coherently in nature and consist of lanthanide elements from La to Lu (International Union of Pure and Applied Chemistry, 2005) [9]. REEs can be divided into light rare earth elements (LREEs; La–Eu) and heavy rare earth elements (HREEs; Gd–Lu). Although Y did not belong to REEs, it was studied together because of its chemically similar behavior to REEs. As significant components of micronutrient elements for plant growth, REEs can activate the endocytosis of plant cells [10]. It was demonstrated in previous studies that during the cultivation of Chinese medicines, e.g., *Ginseng, Coix lachryma-jobi, and Eucommia Land wolfberry,* adding moderate concentrations of rare earth fertilizer notably improved yield, quality and the accumulation of effective constituents [11–14]. These discoveries have led to the large-scale application of rare earth micro-fertilizers to medicines production. In order to enable the development of more sustainable rare earth utilization practices, it is significant to conduct research on their sources, migrations, enrichments, fractionations and transformations in the soil–root environments. Bedrock and its weathering production were the parent materials of soil on which plants survived, which was the natural mineral–nutrition elements pools and primary source of REEs for plants [5,15]. In general, the micronutrient element concentrations in the soils that developed in the mountain terrain were primarily inherited from parent materials. Therefore, the latter controlled the background characteristics of micronutrient elements concentrations in the former [16–18] and, ultimately, the adsorption and enrichments of micronutrient elements in Chinese medicines.

The root of the labiate *Scutellaria baicalensis* was initially documented in *Shennong's Classic of Materia Medica* and in *Collective Notes to the Canon of Materia Medica* as traditional Chinese medicines, which were characterized by a cold property and bitter taste. It is a commonly used Chinese medicine recorded in *The Pharmacopoeia of the People's Republic of China* (2015 version) [19], which is beneficial for clearing away hot and toxic substances, promoting diuresis, cooling blood, preventing miscarriage, and relieving cough [20,21]. Chengde city, Hebei Province, China, has been verified to be one of the top-geoherbs habitats for *Scutellaria baicalensis*. It was claimed in *Differentiation of drug production* that *Scutellaria baicalensis* has been widespread around Zhili and Rehe in Hebei Province for a long time, featuring a thick and long root, solid texture, golden-yellow rind, and extra low impurity, and it has been entitled "Rehe *Scutellaria baicalensis*" [22]. According to a field survey, gneiss was confirmed to be the dominant rock type inhabiting Rehe *Scutellaria baicalensis*. *Scutellaria baicalensis* was also observed being planted in loess locations, and REE-rich micro-fertilizers applications were conducted in parts of these habitats. In order to explore the effect of parent materials on the geoherbalism and quality of *Scutellaria baicalensis* in terms of REEs, three habitats of *Scutellaria baicalensis* with contrasting geo-pedological conditions, i.e., naturally grown habitat (NGHs), artificial planting habitats (APHs) without fertilization, and biomimetic cultivation habitats (BCHs) under field management and fertilization were studied. This study focused on the enrichments and fractionations of REEs during bedrock weathering and micronutrients adsorption by *Scutellaria baicalensis*

and further on the controlling mechanism based on field eco-geological investigation and systematical sampling on roots of *Scutellaria baicalensis* and corresponding rhizosphere soil, and in weathering crust from the bottom of bedrock up to soil. REEs test for all samples and flavonoid compound tests for roots of *Scutellaria baicalensis* were conducted.

2. Physical Geography and Distribution of *Scutellaria baicalensis*

The study area is located in Yanshan Mountain, geographically in Chengde city, Hebei Province, China, where Rehe *Scutellaria baicalensis* is regionally widespread. A warm temperate semi-humid continental monsoon climate characterizes the region, with annual precipitation from 500 to 800 mm, frost-free days from 92 to 180 d, an annual effective accumulative temperature from 2800 to 3980 °C, and annual sunshine duration from 2500 to 3100 h [23]. The characteristics of the three comparable habitats of *Scutellaria baicalensis* (NGHs, APHs, and BCHs) were as follows (Figure 1).

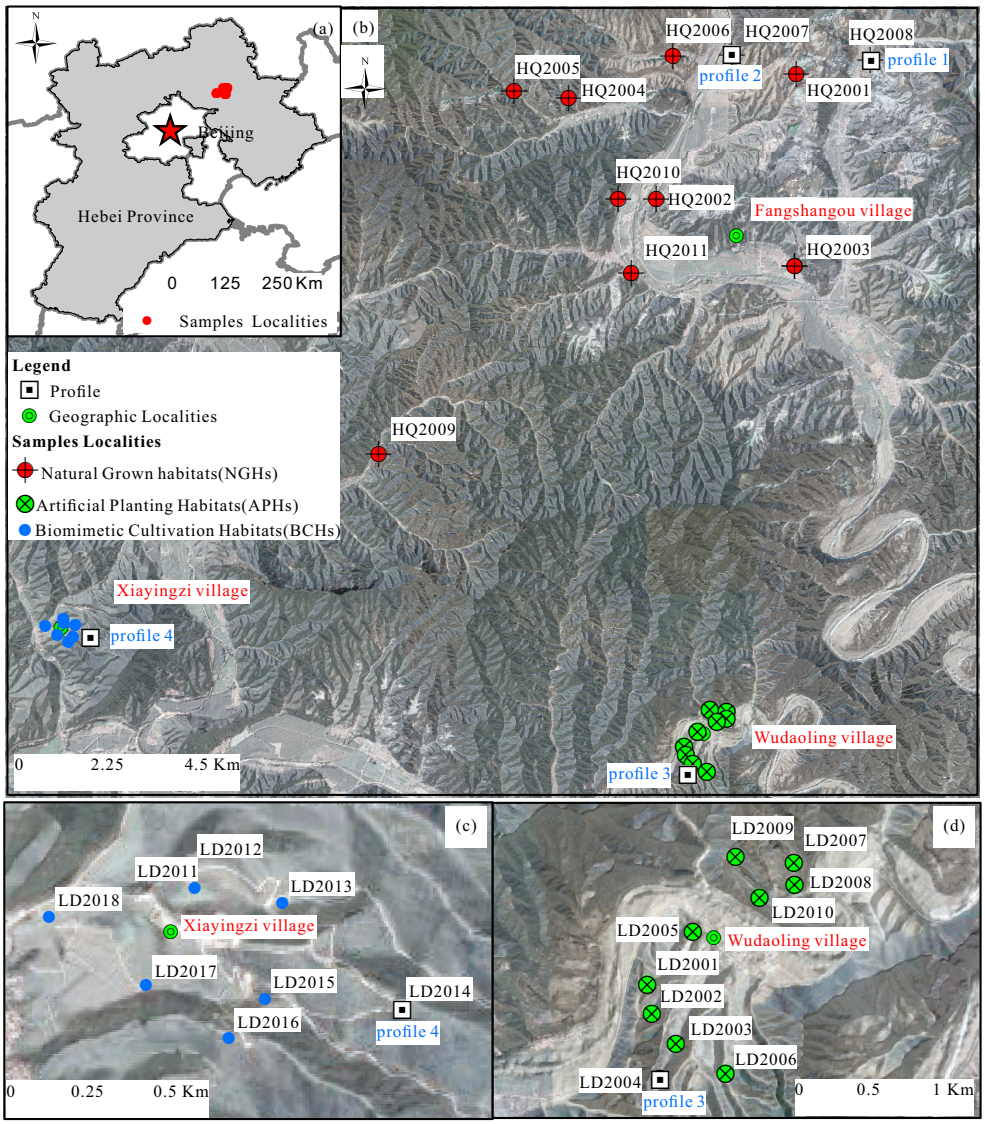

Figure 1. (**a**) Geographical location map; (**b**) Distribution map of sampling in three habitats; (**c**) Distribution map of sampling in biomimetic cultivation habitats (BCHs); (**d**) Distribution map of sampling in artificial planting habitats (APHs).

(1) It was documented that NGHs were concentrated in southern Chengde, such as Luanping County, Xinglong County and Kuanchen County, China. Based on our field survey, NGHs in Hongqi, Luanping County, were selected for sampling (Figure 2a–c).

The lithology was dominated by hornblende-gneiss, which were strongly weathered and had intensive fractures along weathering profiles, resulting in thick saprolite and soil with a thickness of 1 m.

(2) Sample plots of APHs were concentrated in Wudaoling village, Luanping County, whose parent materials were loess. *Scutellaria baicalensis* was planted in artificial terraced fields without fertilization (Figure 2d,e).

(3) Sample plots of BCHs were chosen in a Chinese herbal medicine plantation in Xiayingzi Villiage, Luanping County, whose parent materials were also loess, mingled with a small amount of weathering residues of andesitic volcanic and pyroclastic rocks. *Scutellaria baicalensis* was planted along turnover hillside fields under field management by biomimetic cultivation and adding a certain amount of REE-rich micro-fertilizers to replenish the soil nutrient contents (Figure 2f).

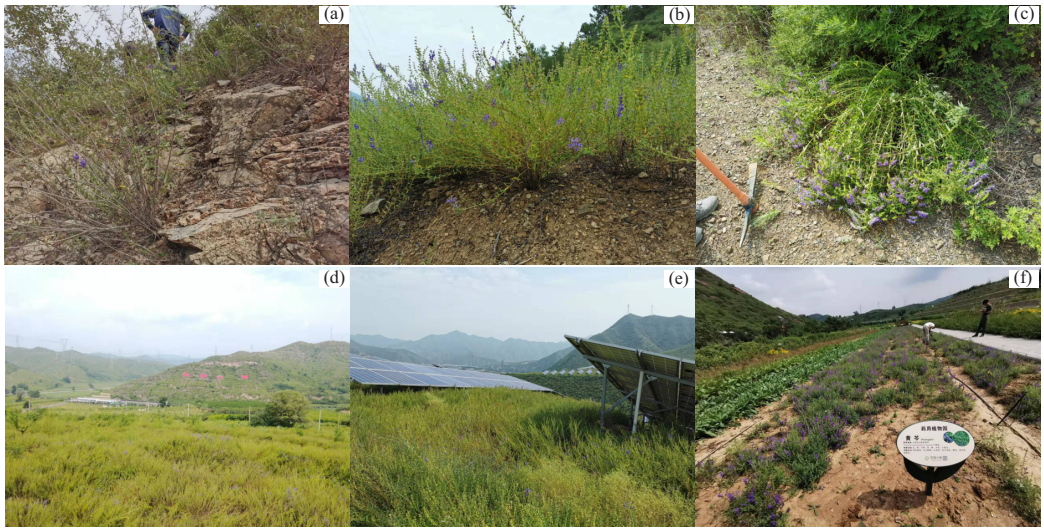

Figure 2. Field photos of *Scutellaria baicalensis* in various habitats; (**a**–**c**) Natural grown habitats (NGHs); (**d**,**e**) Artificial planting habitats (APHs); (**f**) Biomimetic cultivation habitats (BCHs).

3. Materials and Methods

3.1. Sampling Strategy

For research on the migrations and enrichments of REEs in the soil–roots environment, the sampling numbers of rhizosphere soils and corresponding roots of *Scutellaria baicalensis* in NGHs, APHs, and BCHs were 11, 10 and 8, respectively. Soil samples were collected in the topsoil layer extending 20 cm down from the surface. In addition, two weathering profiles in the close vicinity of field plots (HQ2007 and HQ2008) in NGHs were systemically sampled from the fresh parent rock (bedrocks) through the semi-weathered and highly weathered horizons (regoliths) to the fully weathered horizons (soils). Both profiles were distributed in the second stage of Fenghuangzui formation in the Neoarcjean Dantazi group, whose rock type was dominated by migmatite hornblende-gneiss, amphibolite and biotite-plagioclase-fels. In our study, the rock type of both profiles was hornblende-gneiss; however, their mineralogical compositions were slightly different: the bedrock in profile 1 was mainly composed of medium- and coarse-grained hornblende, plagioclase, quartz and a small amount of fine-grained biotite, while in profile 2, the bedrock was mainly composed of fine-grained plagioclase, biotite, quartz, and a small amount of hornblende. Weathering extended to a depth of 3.6 m in profile 1. The soil layer was 20 cm thick, and its texture was dominated by gravel. The regolith layer extended for a further 340 cm below soil layers with the chemical index of alteration (CIA) values ranging from 65.0 to 71.1. Bedrock extended to a depth of 5.6 m. Weathering extended to a depth of 5.8 m in profile 2. The soil layer was 50 cm thick, with the humus horizon being 10 cm. The soil texture was dominated by gravel. The regolith layer extended for a further 530 cm below

soil layers with the CIA values ranging from 51.1 to 67.2. Bedrock extended to a depth of 7.6 m in which alteration zones, e.g., chloritization, occurred, extending 1 m upwards from the bottom. About 1–2 samples were collected per subhorizon. A total of 8 samples from profile 1 and 10 samples from profile 2 were collected, and each one soil profile was collected per habitats in APHs and BCHs in the close vicinity of field plots (LD2004 and LD2014), respectively. The topsoil layer extending 20 cm downwards from the surface and the loess layer extending for a further 20 cm were sampled, and a total of 2 samples from profile 3 and also 2 samples from profile 4 were collected.

3.2. Analytical Methods

For REE analyses, the prepared samples were first dried at 70 °C, and then both the dried soil, regolith and fresh bedrock were crushed, pulverized by an agate mortar and sieved through a 200 mesh into powder. The powder was baked at 105 °C to remove adsorbed water before analysis. REEs were measured using inductively coupled plasma-mass spectrometry (ICP–MS). For soil samples, approximately 50 mg of soil sample was digested with 0.5 mL HNO_3 and 1 mL HF in screw-top, PTFE-lined stainless steel bombs at 185 °C for 24 h. The inner Teflon was removed from the hot plate after cooling, and the solution was evaporated to dryness. The solution was then drained and evaporated to dryness with 0.5 mL HNO_3. This procedure was repeated twice. The final residue was redissolved by adding 1.5 mL HNO_3 and 1.5 mL deionized water. Subsequently, the bomb was resealed and heated at 130 °C for 3 h. After cooling to room temperature, the final solution was diluted to 50 mL by adding distilled deionized water. For regolith and bedrock samples, approximately 50 mg of powdered samples was digested with 100 mL APS, which was followed by mechanical shaking for 2 h and standing for 30 min. After filtration at medium speed, 2 mL of filterable solution was diluted to 100 mL by adding distilled deionized water. Subsequently, 10 mL of the solution was diluted to 100 mL by adding 1 mL indium (In) solution, 1 mL HNO_3 and deionized water. The *Scutellaria baicalensis* samples were washed with tap water and deionized water successively and then oven-dried at 75 °C until the dry weight reached a constant value. Due to the dominant distributions of flavonoid compounds in roots, roots were used for an REE and flavonoid compound test. The dry root samples were ground to a fine powder. Approximately 200 mg of powdered sample was digested with 5 mL HNO_3 in a high-pressure digestion tank for 1 h, which was followed by cooling and removing HNO_3 at 140 °C. After cooling to room temperature, the solution was diluted to 10 mL by adding deionized water. The reagent blanks of soil, regolith, bedrock, and roots were treated following the same procedures as the corresponding samples. The total analytical errors for REEs in this study were within ± 6.

High-Performance Liquid Chromatography (HPLC–DAD) was applied to test the six flavonoid compounds, including baicalin, oroxylin A glycoside, wogonoside, baicalein, wogonin, and oroxylin A. First, the reference substances of the six flavonoid compounds were dissolved in chromatographic methanol and shaken to prepare the reference solution. Second, root powder samples were placed in a volumetric flask with 70% ethanol and shaken. The supernatant was extracted for filtration through a 0.22 μm filter membrane after ultrasonic extraction for 40 min and cooling to room temperature. Finally, a high-performance liquid chromatograph Water E2695 was utilized to test the flavonoid compounds of the reference solutions and our specimens. Methanol-0.1% phosphoric acid solution was applied to gradient elute the mobile phase. The accuracy was controlled by adding 10% of blank samples and parallel samples during testing according to the specification requirement.

3.3. Parameters on the REE Distribution Characteristics

ΣREE, ΣLREE and ΣHREE were calculated as the sum of REEs, LREEs and HREEs, respectively. LREE/HREE was the ratio of ΣLREE to ΣHREE and La_N/Yb_N was the ratio

of La_N and Yb_N, where La_N and Yb_N represent the chondrite normalized values of La and Yb.

Eu anomaly values are quantifed as (1):

$$\delta Eu = \frac{Eu_N}{\sqrt{Sm_N \times Gd_N}}, \quad (1)$$

where Eu_N, Sm_N, and Gd_N represent the chondrite normalized values of Eu, Sm, and Gd, respectively.

Ce anomalies were calculated by formula (2):

$$\delta Ce = \frac{Ce_N}{\sqrt{La_N \times Pr_N}}, \quad (2)$$

where Ce_N, La_N, and Pr_N represent the chondrite normalized values of Ce, La, and Pr, respectively.

The normality of the parameters in various habitats was confirmed using the Shapiro–Wilkes test, and probability (p value) lower than 0.05 showed their abnormal distribution. The normal distribution test was conducted in SPSS 26.0.

4. Results

4.1. REE Concentrations in the Weathering Crust

4.1.1. REE Concentrations of Rhizosphere Soils

The concentrations of REEs and several parameters on the REEs distribution characteristics of rhizosphere soils in various habitats are listed in Table 1. According to the Shapiro–Wilkes test, ΣREE, ΣLREE and ΣHREE in the rhizosphere soils were normally distributed in NGHs and APHs ($p > 0.05$) but not in BCHs ($p < 0.05$), and therefore, the median represents the statistical characteristic of REE concentrations in various habitats. Rhizosphere soils in NGHs contained REE concentrations with the median ΣREE values being 173 $\mu g \cdot g^{-1}$ and the median ΣLREE values being 157 $\mu g \cdot g^{-1}$, which were higher than that in APHs with the median ΣREE values being 149 $\mu g \cdot g^{-1}$ and the median ΣLREE values being 133 $\mu g \cdot g^{-1}$. However, ΣHREE exhibited the opposite feature that rhizosphere soils in APHs with higher HREE concentrations. The median LREE/HREE and La_N/Yb_N of rhizosphere soils in NGHs were 9.76 and 7.86, respectively, which were higher than that in APHs with a median of 11.4 and 8.82, respectively, suggesting greater fractionations with LREEs and HREEs in NGHs. After micro-fertilizers application, it exhibited remarkable enrichments of REEs in the rhizosphere soils of BCHs with the median ΣREE, ΣLREE and ΣHREE values being 187 $\mu g \cdot g^{-1}$, 166 $\mu g \cdot g^{-1}$ and 20.2 $\mu g \cdot g^{-1}$, respectively, which were also higher than that in NGHs. Additionally, LREE/HREE and La_N/Yb_N in the rhizosphere soils of BCHs increased, with the median LREE/HREE and La_N/Yb_N being 8.36 and 9.53, respectively. The chondrite-normalized REE patterns exhibited an obvious right-inclined style that all the rhizosphere soils were enriched in LREEs (Figure 3a,c,e) with moderately to slightly negative Eu anomalies, especially in APHs and BCHs. However, the Ce anomaly was not apparent. The coefficients of variation (CVs) of ΣREE, ΣLREE and ΣHREE of rhizosphere soils in APHs were 6.84%, 6.88% and 8.84%, respectively, which were much lower than those in NGHs and BCHs, indicating that the REEs concentrations of soils developed in loess without fertilization were relatively homogeneous.

4.1.2. REE Concentrations in the Weathering Profile

Two weathering profiles were distributed in hornblende-gneiss locations. The ΣREE values of bedrock were 233 $\mu g \cdot g^{-1}$ and 264 $\mu g \cdot g^{-1}$, respectively, in profiles 1 and 2, indicating their similar REEs concentrations. Both weathering profiles in NGHs showed similar chondrite-normalized REE patterns from the bottom of bedrock up to regolith, and onto the soil, with enrichment of LREEs and moderately negative Eu anomalies (Table 2, Figure 4), which is in accordance with the weathering characteristics in mountain terrain that bedrock was in-situ weathered to the soil, and the latter has inherited REE concentrations from the

former. However, different enrichments and fractionations within REEs have occurred during weathering. As shown in profile 1 (Figure 4a), the ΣREE was overall higher in the regoliths in which HREEs were deficient, but LREEs were enriched as compared to bedrock, while topsoil was deficient in both LREEs and HREEs. Regoliths contained higher REE concentrations with ΣREE values ranging 242–289 $\mu g \cdot g^{-1}$, and that of soil was 169 $\mu g \cdot g^{-1}$. LREE/HREE varied in the range of 8.28–11.2 and La_N/Yb_N varied in the range of 9.24–13.8, which were slightly different with bedrock (LREE/HREE = 8.56, La_N/Yb_N = 9.48). However, profile 2 exhibited that the ΣREE was overall lower in the regoliths and soils, and that LREEs were more deficient than HREEs in both regolith and soil as compared to bedrock, while topsoil was more enriched in REEs than regolith (Figure 4b). Regoliths contained lower REE concentrations with ΣREE values ranging 142–238 $\mu g \cdot g^{-1}$, and that of topsoil was 238 $\mu g \cdot g^{-1}$. LREE/HREE varied in the range of 6.08–10.7 and La_N/Yb_N varied in the range of 5.83–14.3, which were different with bedrock (LREE/HREE = 20.6, La_N/Yb_N = 35.8).

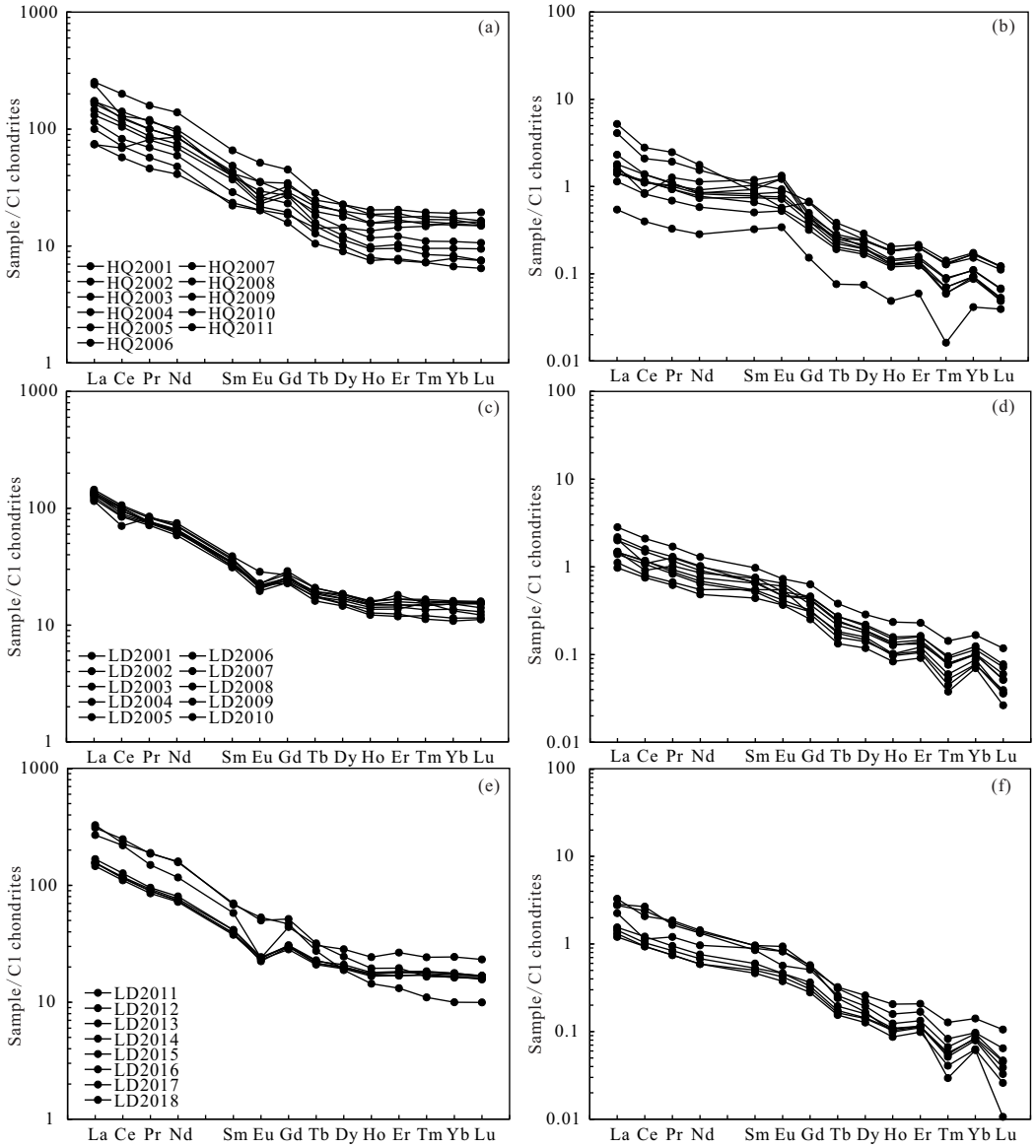

Figure 3. Chondrite-normalized REE patterns of rhizosphere soils and roots of *Scutellaria baicalensis*. (**a**) Rhizosphere soils in NGHs; (**b**) Roots in NGHs; (**c**) Rhizosphere soils in APHs; (**d**) Roots in APHs; (**e**) Rhizosphere soils in BCHs; (**f**) Roots in BCHs.

Table 1. Parameters on REE distribution characteristics of rhizosphere soils in various habitats, Hebei Province.

Parameters	Habitats	Median (25–75%) ($\mu g \cdot g^{-1}$)	Average ($\mu g \cdot g^{-1}$)	Skewness	CV/%	*p* Value
ΣREE	NGHs (n = 11)	174 (127–212)	173	0.754	33.9	0.541
	APHs (n = 10)	149 (140–156)	149	0.231	6.84	0.753
	BCHs (n = 8)	187 (177–337)	238	0.726	34.4	0.007
ΣLREE	NGHs (n = 11)	154 (115–194)	157	0.765	35.1	0.673
	APHs (n = 10)	133 (124–139)	133	0.120	6.88	0.791
	BCHs (n = 8)	166 (158–311)	216	0.761	36.8	0.009
ΣHREE	NGHs (n = 11)	15.2 (12.1–19.9)	16.2	0.131	29.7	0.802
	APHs (n = 10)	16.7 (15.3–18.1)	16.6	−0.158	8.84	0.701
	BCHs (n = 8)	20.2 (19.5–24.7)	21.7	1.49	16.3	0.008
LREE\HREE	NGHs (n = 11)	9.76 (7.85–11.5)	9.85	0.156	25.2	0.814
	APHs (n = 10)	7.86 (7.64–8.30)	8.01	1.89	7.00	0.016
	BCHs (n = 8)	8.36 (7.96–11.7)	9.84	1.73	29.8	0.005
$La_N \backslash Yb_N$	NGHs (n = 11)	11.4 (8.49–15.9)	12.4	1.03	46.0	0.315
	APHs (n = 10)	8.82 (8.34–10.1)	9.27	1.37	12.7	0.042
	BCHs (n = 8)	9.53 (8.87–17.6)	13.4	1.96	59.7	0.001
δEu	NGHs (n = 11)	0.900 (0.710–0.970)	0.869	−0.168	14.4	0.385
	APHs (n = 10)	0.719 (0.704–0.791)	0.743	1.31	8.05	0.057
	BCHs (n = 8)	0.686 (0.652–0.793)	0.699	0.032	18.9	0.512
δCe	NGHs (n = 11)	0.950 (0.890–0.970)	0.919	−2.09	8.15	0.002
	APHs (n = 10)	0.910 (0.870–0.935)	0.892	−2.20	7.89	0.003
	BCHs (n = 8)	0.950 (0.935–0.990)	0.959	0.490	5.18	0.510

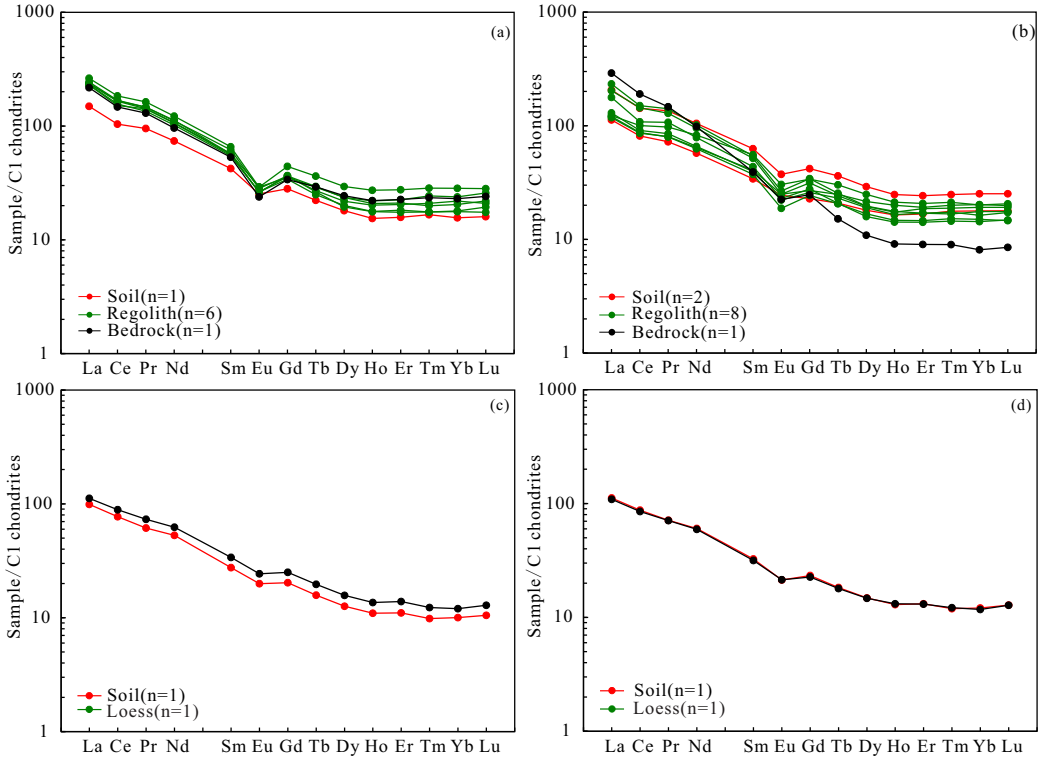

Figure 4. Chondrite-normalized REE patterns of layers along profiles. (**a**) Chondrite-normalized REE patterns along profile 1 in NGHs; (**b**) Chondrite-normalized REE patterns along profile 2 in NGHs; (**c**) Chondrite-normalized REE patterns along profile 3 in APHs; (**d**) Chondrite-normalized REE patterns along profile 4 in BCHs.

Soils developed in loess also showed chondrite-normalized REE patterns similar to those of parent materials with enrichment of LREEs and lightly negative Eu anomalies (Figure 4c,d). It also exhibited the depletion of REEs in topsoil as compared to parent material in APHs. The ΣREE values of parents materials (loess) were similar, 139 and 133 $\mu g \cdot g^{-1}$, whose corresponding soils contained total REE concentrations being 119 and 136 $\mu g \cdot g^{-1}$. LREE/HREE was, respectively, 8.43 and 8.17, which was similar to their parent materials with LREE/HREE being 7.90 and 8.11. La_N/Yb_N was, respectively, 9.87 and 9.23, which was similar to their parent materials, with La_N/Yb_N being 9.32 and 9.26. In general, the REEs of soils and parent material horizons in hornblende-gneiss were more abundant, and they had more substantial variation between LREE and HREE than those in loess.

Table 2. Parameters on REEs distribution characteristics along profiles in various habitats, Hebei Province.

Habitats	Profile	Layer	Depth (cm)	ΣREE ($\mu g \cdot g^{-1}$)	ΣLREE ($\mu g \cdot g^{-1}$)	ΣHREE ($\mu g \cdot g^{-1}$)	LREE/HREE	La_N/Yb_N	δEu	δCe
NGHs (hornblende gneiss)	Profile 1	Soil	0–20	169	150	18.2	8.28	9.52	0.734	0.872
		regolith	20–30	259	235	23.8	9.88	11.6	0.596	0.895
		regolith	50–70	259	237	21.2	11.2	13.8	0.572	0.889
		regolith	260–270	255	231	24.6	9.37	9.9	0.650	0.902
		regolith	280–300	243	220	23.2	9.47	10.5	0.587	0.842
		regolith	310–320	289	259	30.3	8.54	9.24	0.538	0.888
		regolith	340–360	242	221	21	10.5	12.9	0.612	0.883
		bedrock	540–560	233	208	24.4	8.56	9.48	0.563	0.875
	Profile 2	soil	0–10	238	210	28.3	7.4	8.19	0.729	0.852
		soil	20–40	134	117	17.7	6.6	6.31	0.879	0.901
		regolith	60–80	238	218	20.4	10.6	14.3	0.619	0.827
		regolith	110–120	146	126	20.7	6.08	5.83	0.756	0.883
		regolith	210–220	151	132	18.6	7.11	7.36	0.693	0.867
		regolith	230–240	172	149	23.5	6.32	6.11	0.700	0.918
		regolith	290–300	142	126	16.6	7.55	8.01	0.621	0.890
		regolith	510–520	180	163	16.9	9.67	12.4	0.660	0.783
		regolith	560–580	223	202	20.6	9.81	10.6	0.620	0.889
		Bedrock	600	264	252	12.2	20.6	35.8	0.724	0.921
APHs (loess)	profile 3	soil	0–20	119	107	12.6	8.43	9.87	0.841	0.990
		loess	20–40	139	124	15.6	7.90	9.32	0.835	0.982
BCHs (loess)	profile 4	soil	0–20	136	121	14.8	8.17	9.23	0.775	0.981
		loess	20–40	133	118	14.6	8.11	9.26	0.799	0.968

4.2. REE Concentrations in the Roots of Scutellaria baicalensis

The concentrations of REEs and several parameters on the REE distribution characteristics for roots of *Scutellaria baicalensis* in various habitats are listed in Table 3. The median was also utilized to represent the statistical characteristic of REE concentrations in the roots of various habitats. Roots of *Scutellaria baicalensis* contained similar ΣREE and ΣLREE in NGHs (ΣREE = 2.02 $mg \cdot kg^{-1}$, ΣLREE = 1.78 $mg \cdot kg^{-1}$) and BCHs (ΣREE = 2.04 $mg \cdot kg^{-1}$, ΣLREE = 1.82 $mg \cdot kg^{-1}$), which are higher than that in APHs (ΣREE = 1.78 $mg \cdot kg^{-1}$, ΣLREE = 1.60 $mg \cdot kg^{-1}$). However, roots in NGHs contained the highest HREE concentrations, with the median ΣHREE being 0.212 $mg \cdot kg^{-1}$, and roots in BCHs contained the lowest HREE concentrations, with the median ΣHREE being 0.183 $mg \cdot kg^{-1}$, which was exactly opposite to the ΣHREE in the soils. LREE/HREE and La_N/Yb_N decreased following the order of BCHs > APHs > NGHs, which was inconsistent with the order in the soils. The considerable variance in REEs adsorption by roots from the rhizosphere soil between various habitats can be speculated. The concentrations of REEs with even atomic numbers were higher than those with odd atomic numbers at HREEs, which conformed to the rule of Oddo-Harkins [24,25]. In general, the chondrite-normalized REE patterns presented an obvious right-inclined style with the enrichment of LREEs (Figure 3b,d,f). Positive Eu anomalies were observed for some samples in all habitats, indicating the adsorption of Eu from soil to some extent. However, the negative Ce anomaly of roots was stronger than that of soil, especially in NGHs, since Ce^{4+} was hard to be adsorbed by roots.

Table 3. Parameters of the REE distribution characteristics of *Scutellaria baicalensis* in various habitats, Hebei Province.

Parameters	Habitats	Median (25–75%) ($mg \cdot kg^{-1}$)	Average ($mg \cdot kg^{-1}$)	Skewness	CV/%	*p* Value
ΣREE	NGHs (*n* = 11)	2.02 (1.79–2.3)	2.21	1.14	47.0	0.066
	APHs (*n* = 10)	1.78 (1.55–2.31)	1.94	1.01	30.3	0.484
	BCHs (*n* = 8)	2.04 (1.5–3.33)	2.34	0.386	38.0	0.042
ΣLREE	NGHs (*n* = 11)	1.78 (1.62–2.11)	2.00	1.24	49.2	0.056
	APHs (*n* = 10)	1.6 (1.4–2.09)	1.76	0.998	30.7	0.491
	BCHs (*n* = 8)	1.82 (1.36–3.12)	2.15	0.441	39.8	0.039
ΣHREE	NGHs (*n* = 11)	0.212 (0.175–0.246)	0.209	−0.541	30.3	0.724
	APHs (*n* = 10)	0.187 (0.146–0.217)	0.187	1.07	28.1	0.376
	BCHs (*n* = 8)	0.183 (0.148–0.235)	0.189	0.378	25.7	0.580
LREE\HREE	NGHs (*n* = 11)	8.64 (7.55–10.8)	9.27	1.48	23.7	0.063
	APHs (*n* = 10)	9.27 (8.57–9.89)	9.38	0.840	11.0	0.536
	BCHs (*n* = 8)	10.2 (9.13–14.7)	11.27	0.556	26.2	0.283
$La_N \backslash Yb_N$	NGHs (*n* = 11)	15.2(12.4–20.9)	17.26	1.07	43.4	0.291
	APHs (*n* = 10)	16 (14.6–18.4)	16.56	1.04	15.0	0.246
	BCHs (*n* = 8)	19.8 (16.5–32.9)	24.58	1.10	43.6	0.168
δEu	NGHs (*n* = 11)	1.28 (1.08–1.57)	1.32	−0.109	22.8	0.985
	APHs (*n* = 10)	0.937 (0.854–1.14)	0.998	0.787	16.0	0.185
	BCHs (*n* = 8)	1.06 (0.972–1.13)	1.05	−0.357	11.6	0.972
δCe	NGHs (*n* = 11)	0.9 (0.730–0.950)	0.845	−1.00	15.7	0.192
	APHs (*n* = 10)	0.935 (0.858–0.963)	0.897	−1.55	12.5	0.009
	BCHs (*n* = 8)	0.935 (0.835–1.04)	0.933	−0.241	16.7	0.933

4.3. Accumulation of REE in the Roots of Scutellaria baicalensis

The biological absorption coefficient (BAC) of REEs provides an estimate of the individual availability of REEs to the plant [26–28]. This was adopted to quantify the natural process of element transfer from the soil to the roots of *Scutellaria baicalensis*. The BAC is defined as follows (3):

$$BAC_i = \frac{CM_i}{CS_i}, \quad (3)$$

where BAC_i is the migration and accumulation rate of element i, and CM_i and CS_i are the concentrations of element i in the plant and soil, respectively. The results were categorized into five groups based on the magnitude of the coefficient: BAC > 3—very strongly accumulated; from 1.5 to 3.0—strongly accumulated; from 0.5 to 1.5—moderate absorption; from 0.1 to 0.5—weak absorption, and BAC < 0.1—very weak absorption [29]. Under normal circumstances, the ratio of the concentrations of REEs in plants to that in the soil is less than 1, even as low as 0.02 [30]. In the study area, all REEs in *Scutellaria baicalensis* had low BACs: less than 0.1.

One-way ANOVA and LSD tests were applied to analyze whether there were remarkable differences in the BACs of REEs between various habitats after the test for normal distribution and homogeneity of variance. In addition, permutation tests, t tests and nonparametric tests were utilized for the BACs that were not normally distributed or had heterogeneity of variance. The statistical analyses were conducted in the R program. In the box plots, various letters (e.g., a and b) imply that there exist statistically remarkable differences between BACs in various habitats ($p < 0.05$); otherwise, differences are not statistically remarkable(e.g., ab and a, ab and b). Almost all HREEs and Y, except for Gd and

Tb, showed statistically remarkable differences in BACs between NGHs with both BCHs and APHs. According to the median (black line in the box), the BACs of all REEs decreased in the order of NGHs > APHs > BCHs (Figure 5), suggesting higher utilization efficiency for REEs with natural source from bedrock, which was attributed to their self-adaption to the environment for a long time in a complicated open system [31]. On the contrary, the utilization efficiency for anthropogenic REEs was relatively low.

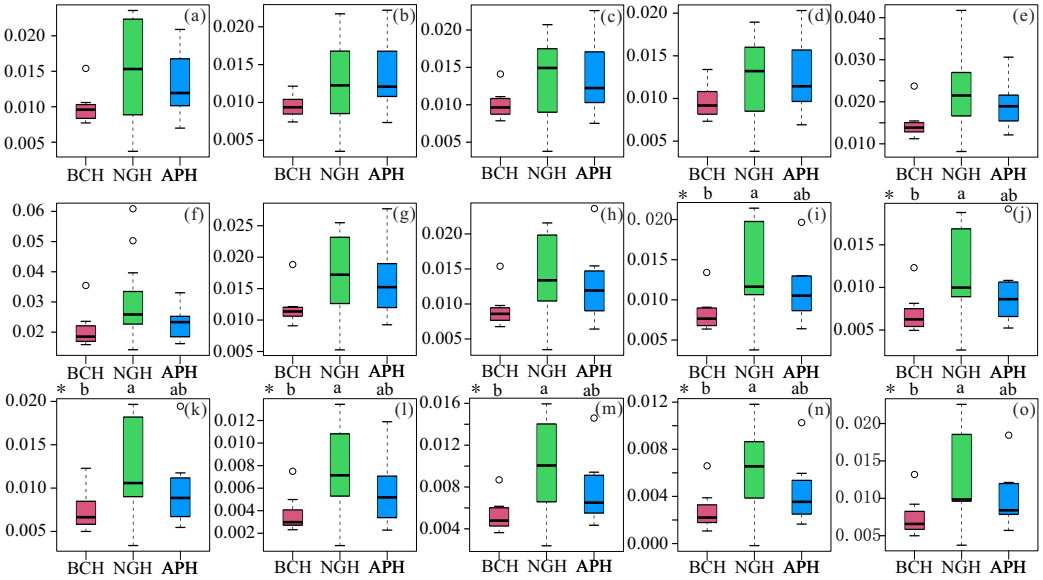

Figure 5. Box plot of biological absorption coefficient (BACs) of REEs Y from soils into roots. (**a**) La; (**b**) Ce; (**c**) Pr; (**d**) Nd; (**e**) Sm; (**f**) Eu; (**g**) Gd; (**h**) Tb; (**i**) Dy; (**j**) Ho; (**k**) Er; (**l**) Tm; (**m**) Yb; (**n**) Lu; (**o**) Y. * $p < 0.1$.

4.4. Effective Constituent Content of Scutellaria baicalensis

Flavonoid compounds are the dominant effective constituents of *Scutellaria baicalensis*, which are composed of two polyhydroxy phenolic benzene rings interconnected by three carbon atoms. Flavonoid compounds included baicalin, oroxylin A glycoside, wogonoside, baicalein, wogonin, and oroxylin A, in which baicalin was recognized as the main criterion of quality [32]. Contents of baicalin ranged from 12.8 to 51.7 mg·g^{-1} with an average of 27.5 mg·g^{-1} in the NGHs, which were higher than that in APHs (4.22–13.2 mg·g^{-1}) and BCHs (4.04–17.1 mg·g^{-1}). Almost all the flavonoid compounds were normally distributed ($p > 0.05$) except for oroxylin A in BCHs. According to the average, baicalin and wogonoside decreased in the order of NGHs > BCHs > APHs, and oroxylin A glycoside, baicalein, wogonin, and oroxylin A followed the order of NGHs > APHs > BCHs (Table 4).

Table 4. Statistical characteristics of flavonoid compound contents in the roots of *Scutellaria baicalensis*.

Flavonoids Compounds	Habitats	Average (mg·g^{-1})	Ranges (mg·g^{-1})	Skewness	*p* Value
Baicalin	NGHs (n = 11)	27.5	12.8-51.7	1.42	0.325
	APHs (n = 10)	8.28	4.22–13.2	0.546	0.911
	BCHs (n = 8)	11.0	4.04–17.1	−0.411	0.273
Oroxylin A glycoside	NGHs (n = 11)	1.85	0.270-4.03	1.06	0.326
	APHs (n = 10)	0.895	0.030–1.83	0.136	0.601
	BCHs (n = 8)	0.724	0.080–1.62	0.633	0.726

Table 4. *Cont.*

Flavonoids Compounds	Habitats	Average ($mg \cdot g^{-1}$)	Ranges ($mg \cdot g^{-1}$)	Skewness	*p* Value
Wogonoside	NGHs (n = 11)	5.24	1.96-12.2	1.79	0.099
	APHs (n = 10)	1.81	0.080–3.02	−0.588	0.396
	BCHs (n = 8)	2.69	1.03–4.56	0.031	0.585
Baicalein	NGHs (n = 11)	2.43	0.820–4.68	0.765	0.605
	APHs (n = 10)	1.15	0.550–2.09	1.42	0.356
	BCHs (n = 8)	1.09	0.330–2.43	1.22	0.357
wogonin	NGHs (n = 11)	0.966	0.310–1.75	0.476	0.508
	APHs (n = 10)	0.468	0.200–0.810	0.862	0.598
	BCHs (n = 8)	0.478	0.090–1.19	1.38	0.301
Oroxylin A	NGHs (n = 11)	0.386	0.200–0.560	−0.036	0.61
	APHs (n = 10)	0.23	0.060–0.440	0.378	0.561
	BCHs (n = 8)	0.184	0.030–0.570	1.92	0.031

5. Discussions

5.1. Lithological Influences on the Enrichments and Fractionations of REEs in the Soils

Micronutrient element concentrations in the soils developed in mountain terrain were primarily inherited from parent materials [16–18]. As mentioned, REE distribution patterns of soils developed in different habitats presented a genetic relationship with their corresponding parent materials. According to 1:250,000 reports of regional geologic survey and our field survey, the protolith of hornblende-gneiss in NGHs was femic volcanic rock, whose REEs concentrations were higher than those that developed in loess; therefore, soils developed from hornblende-gneiss contained higher REEs concentrations (ΣREE = 174 $ug \cdot g^{-1}$) than that from loess (ΣREE = 149 $ug \cdot g^{-1}$), which is in agreement with the expectations from the different lithologies that soils originating from volcanic rock tend to have higher REE concentrations than soils developed from loess [28,33,34].

Weathering crust in hornblende-gneiss showed great variation of REEs concentrations than loess, resulting in relatively homogeneous REEs concentrations in the soils developed from loess (CV = 6.84%) and notable heterogeneity of REEs concentrations in the soils developed from hornblende-gneiss (CV = 33.9%). The weathering of parent materials profoundly impacted the migrations and enrichments of REEs. The REE concentrations distribution pattern in soils of loess was significantly similar to their parent materials since their weak weathering and indistinctive movement of clay particles. However, the complex mineral compositions and grain sizes in hornblende-gneiss significantly influenced the weathering process, resulting in remarkable discrepancies in migrations and enrichments of REEs during weathering [35,36]. Two weathering profiles in hornblende-gneiss locations exhibited different evolution of REEs. In profile 1, REE concentrations decreased in the order of soils $<$ bedrock $<$ regoliths, while in profile 2, REE concentrations decreased followed the order regoliths $<$ topsoil $<$ bedrock (Figure 6a,b). It can be speculated that in profile 1, as eluviation proceeded, soluble components were greatly leached while sparingly soluble components, including REEs, showed relative enrichments, resulting in the overall REE enrichments of the regoliths [37,38]. REEs in the topsoil penetrated downward to the lower part of the profile, which was accompanied with REE-containing clay minerals [39,40], resulting in depletion in the topsoil compared with the lower parts. However, the minerals grain size in the bedrock of profile 2 was much smaller than that in profile 1. As the mineral grain size decreases and specific surface area increases, fine-grained rock offers a potentially increased area over which water penetration may occur [41,42]. Therefore, the reaction with water in the regolith and soils causes releasing of REE from REE-containing minerals and the leaching of REE, especially LREE. It was observed in the field that the humus horizon was 10 cm thick with a higher content of organic materials in profile 2; therefore,

topsoil contained higher REE concentrations since organic matter has a fixed effect on REEs [43–45].

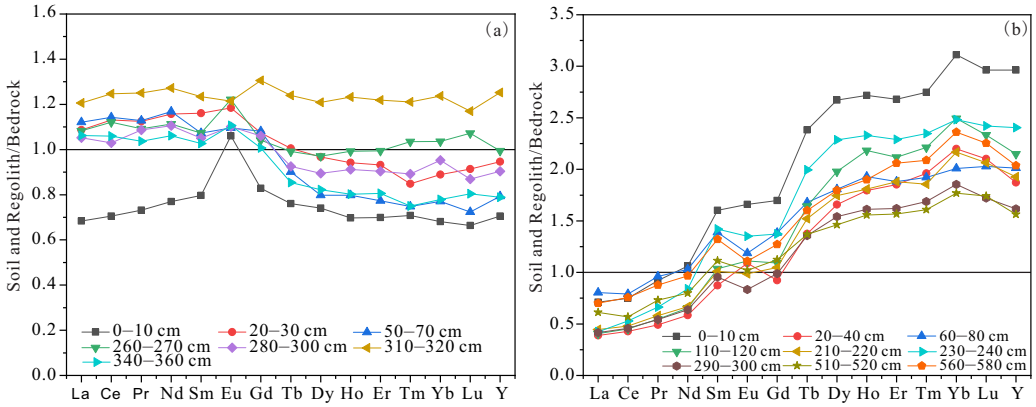

Figure 6. Bedrock-normalized REE patterns in profiles in NGH. (**a**) Profile 1; (**b**) Profile 2.

The clays and iron (hydro) oxide that formed during chemical weathering in hornblende-gneiss locations were notably different, resulting in apparent different fractionations within REEs [46–50], since the mixed speciation of the REEs in clays and Fe-Mn oxyhydroxides is typical for REEs in soils [38,51–53]. Under natural pH, clay minerals with a negative layer charge are effective in the adsorption of REEs through ion exchange, surface complexation, electrostatic attraction and migration into clay structures [54]. The adsorption capacity is largely determined by the surface structure, surface charge of clay minerals and composition [55,56]. In our study area, under alkaline conditions (pH > 7) with abundant Fe^{2+}, Mg^{2+}, and K^{+}, clay minerals were dominated by smectite, illite or chlorite, especially in profile 2 [46,50,57,58]. Smectite and illite may intrinsically retain HREE more efficiently than LREE [46,58]. As shown in Figure 7a, LREE/HREE had a remarkable positive relationship with $SiO_2/(Al_2O_3+Fe_2O_3)$ in profile 2 according to Pearson correlation analysis. As weathering proceeded, clay minerals were gradually generated from aluminosilicate minerals with the enrichment of Al_2O_3 and depletion of SiO_2. In addition, enhanced oxidation contributed to the enrichment of Fe_2O_3. Therefore, the decrease of the $SiO_2/(Al_2O_3+Fe_2O_3)$ ratio showed the enrichment of clay mineral (smectite and illite) and iron (hydro) oxide, favoring the preferential adsorption of HREE and fractionation within REEs [59]. However, according to CIA, the chemical weathering in profile 1 (CIA = 65.0–71.1) was generally stronger than that in profile 2 (CIA = 51.1–67.2), and a small amount of kaolinite and boehmite with higher maturity was formed from illite/smectite [60]. Therefore, LREEs were preferentially adsorbed by kaolinite in profile 1. In addition, HREEs have a smaller ionic radius and stronger hydrolysis ability than LREEs and therefore have a higher affinity toward iron (hydro) oxide. Previous studies also showed that the chondrite-normalized iron (hydro) oxide fractions are slightly enriched in HREEs via inner-sphere complexation and may play an important role in redistributing HREEs in the weathering crust [61,62]. As shown in Figure 7b, LREE/HREE had a remarkable negative relationship with Fe_2O_3 in profile 2, suggesting the critical control of iron (hydro) oxide on the REE fractionation. In the study area, profile 2 contained more abundant Fe_2O_3 (4.92–9.49%, 7.95%) than those in profile 1 (Fe_2O_3 = 4.40–7.47%, 6.22%). Therefore, in profile 1, HREEs are predominantly dissolved and migrate as bicarbonate and organic complexes in solution in case of the low contents of iron (hydro) oxide, leading to the fractionation of REEs among weathering crust [63–69]. However, the preferential scavenging of HREEs during the precipitation of pedogenetic iron (hydro) oxide resulted in the HREE enrichment in profile 2 instead of being dissolved and migrating as bicarbonate and organic complexes, which is consistent with the conclusion of Land (1999) [51].

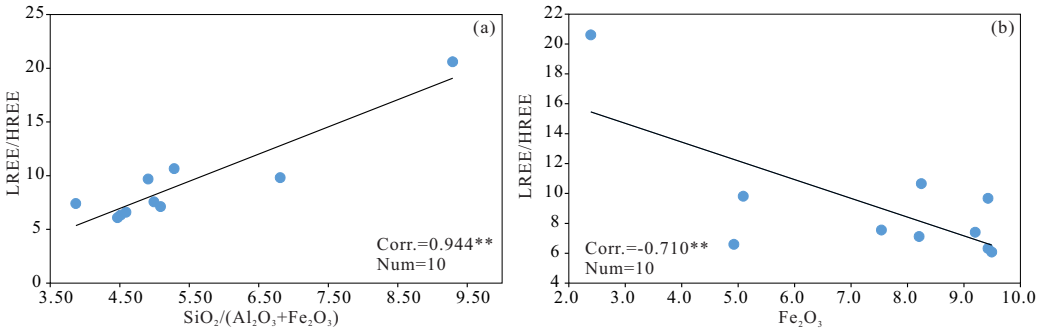

Figure 7. Scatter diagram of (**a**) $SiO_2/(Al_2O_3+Fe_2O_3)$ versus LREE/HREE and (**b**) Fe_2O_3 versus LREE/HREE in profile 2. ** $p < 0.01$.

5.2. Enrichments and Fractionations of REE in the Roots of Scutellaria baicalensis

The soil mineral particles present in the close vicinity of the roots were the primary source of REEs for plants. It exhibited a remarkable positive correlation between ΣREE in the roots and rhizosphere soils with a coefficient of 0.479 ($p < 0.01$), especially the correlation coefficient between ΣLREE in the roots and rhizosphere soils being 0.511 ($p < 0.01$) (Figure 8). Previous research on the distribution of *Scutellaria baicalensis* demonstrated that they were naturally widespread in the fertile sand or loam underlying the humus horizon, especially chestnut soil or sandy loam, with pH values ranging from 5 to 8 [70]. For a type of species, the REEs concentrations in plants are influenced by some complex related factors, including total REEs concentrations and their occurrences in the rhizosphere soils, as well as pH, Eh, clay fraction contents, nutrient features, etc., in the soil–root environment [71–75]. In our study area, the clay fraction contents of soil developed in NGHs range from 18.8 to 66.9 g/kg, and the sand fraction contents range from 884.1 to 940.9 g/kg (our unpublished data), suggesting that soils were classified into sand according to texture classification. Their pH value varied from 7.31 to 8.57, with an average of 8.06. Therefore, NGHs were optimal for the inhabitation of *Scutellaria baicalensis*, and the absence of clay fraction favored the migrations of REEs into plants, resulting in higher biological absorption coefficients (BACs) of REEs. On the contrary, loess in APHs was generally deemed to comprise higher clay fractions than other lithologies. REEs may be preferentially involved in the crystal lattice of clay minerals as isomorphisms or hosted into REE-rich minerals, e.g., Ti oxides or phosphorite, and therefore inhibit the absorption of REEs into plants [37,76], leading to lower BACs of REEs. However, after rare earth micro-fertilizers application, BACs of all REEs in BCHs were still lower than that in APHs, despite both rhizosphere soils and roots in BCH comprised higher REE concentrations. Previous studies have demonstrated that once exogenous REEs enter the soil, more than 99.5% of them are absorbed by the solid phase of the soil, and only a small amount is dissolved in the water present in the soil [10,77]. This means that within a short period, REE fertilization would not notably increase the concentrations of REEs with high bioavailability [78–82], e.g., water-soluble fractions and iron-exchangeable fractions. In contrast, REEs accumulate in the soil as residue fractions, which are difficult for the plant to adsorb [83]. We can conclude that REE fertilization in BCHs contributes to improving REE concentrations in roots to some extent but that utilization efficiency for anthropogenic REEs was relatively low.

The BCAs of LREEs for *Scutellaria baicalensis* were overall higher than those of HREEs. Previous studies showed that the coprecipitation of rare earth ion salts (mostly in the form of insoluble oxalates or phosphates) and the selective absorption of root cell walls (in the form of trivalent cations) were the main mechanisms through which plant roots fix REEs [10,84,85]. In general, the dominant speciation of the LREEs is as free ions, whereas the HREEs are mainly present as dissolved complexes [38,86,87]. Diffusion through ion channels, i.e., passive diffusion, was the dominant movement mechanism of REEs from the soil into the roots [88–90], and LREEs were dominantly adsorbed into root cells in the form of trivalent cations. In this study area, the BACs distribution patterns of REEs in various

habitats exhibited an overall right-inclined style to different degrees, with a high biological absorption coefficient of Eu (Figure 9), indicating that *Scutellaria baicalensis* preferentially adsorbed LREEs and thus resulted in fractionation within REEs.

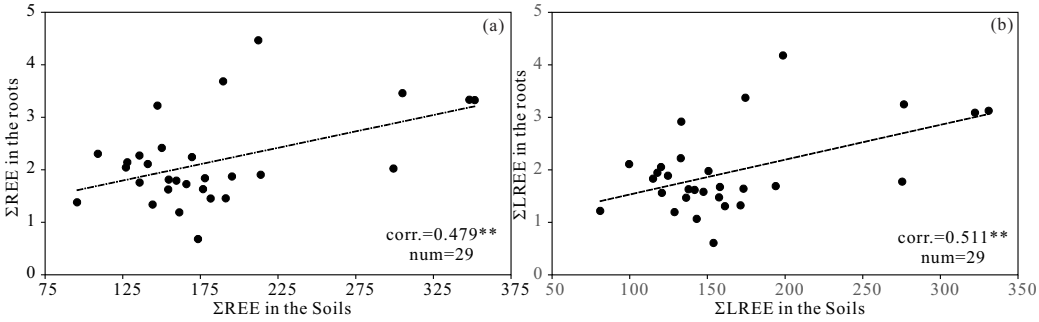

Figure 8. Scatter diagram of (**a**) ΣREE in the rhizosphere soils versus roots and (**b**) ΣLREE in the rhizosphere soils versus roots. ** $p < 0.01$.

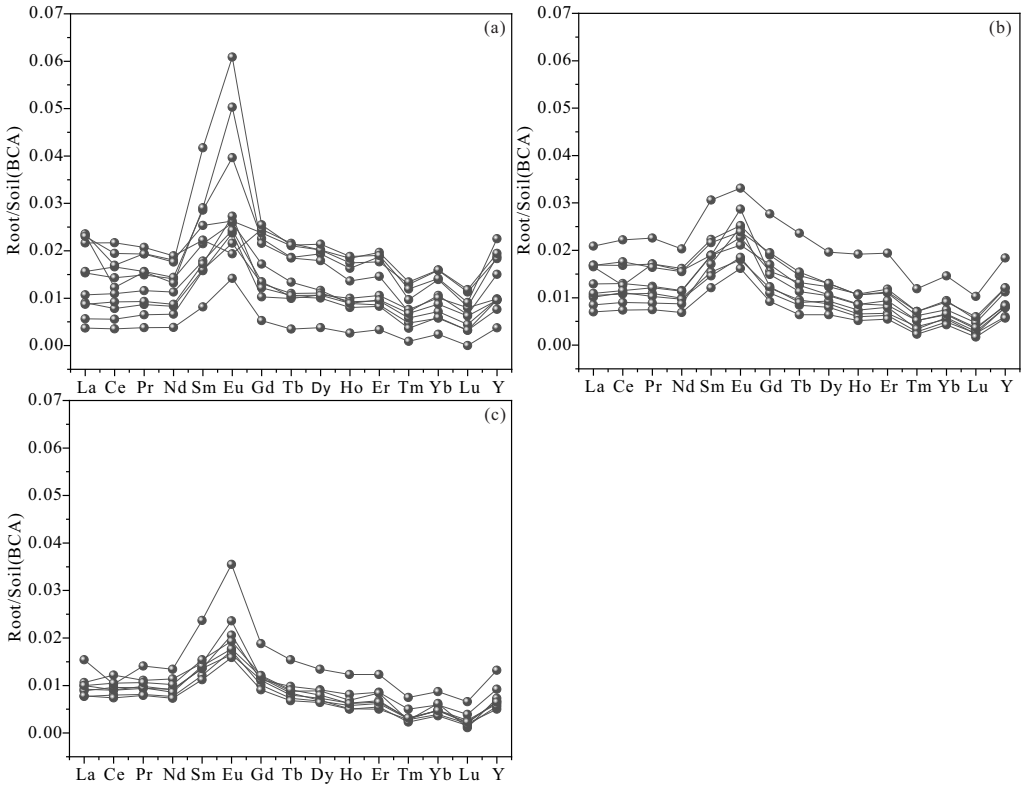

Figure 9. BACs distribution patterns of REEs in roots of *Scutellaria baicalensis*. (**a**) NGHs; (**b**) APHs; (**c**) BCHs.

5.3. Relationships between REE and Effective Constituents of Scutellaria baicalensis

Flavonoid compounds are effective constituents and secondary metabolites of *Scutellaria baicalensis*, which are controlled by the growing conditions, including illumination, temperature, moisture, and nutrients [91]. In our study area, flavonoid compounds were more abundant in NGHs than APHs and BCHs. Previous data have demonstrated that mineral nutrient elements (e.g., REE^{3+}) control the synthesis and accumulation of flavonoid compounds, either as catalysts for secondary compound metabolism [92–96], by involving in their functional structure [97–100] or by contributing to the growth of cells [101–105]. Pearson correlation analysis was applied to check out further the correlations between micronutrient elements with flavonoid compounds in the roots. The results exhibited that micronutrient elements, including REEs, Cu, Zn, Sr, Ge, and Se, had a significant positive

correlation with flavonoid compounds to some extent ($p < 0.05$ or $p < 0.01$) (Figure 10), indicating that the micronutrient elements of roots have a significant influence on the medicinal composition of *Scutellaria baicalensis*.

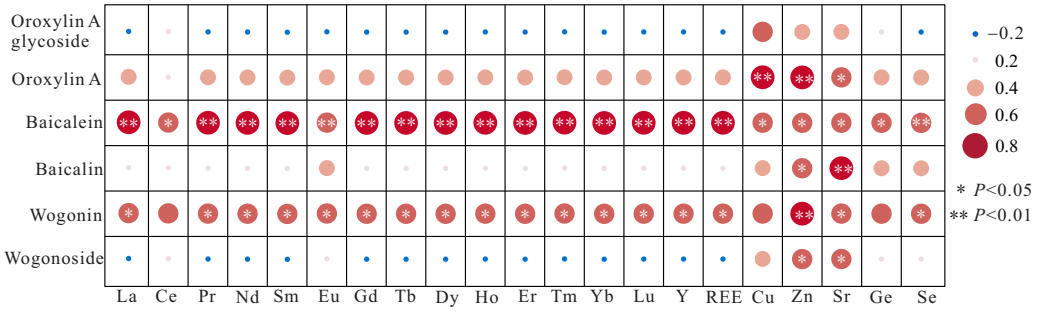

Figure 10. Pearson correlation analysis between flavonoid compounds and micronutrient elements in the roots of *Scutellaria baicalensis*.

It was widely acknowledged that the activation of endocytosis is the primary response of plant cells to REEs [10,106–108], which induces a series of physiological and biochemical responses, affecting the activation of various enzymes, substance synthesis and cell growth [104,107,109,110]. Previous studies have demonstrated that exposure to REEs can affect the absorption of mineral elements by plants [111,112]. In our study area, roots of *Scutellaria baicalensis* in NGHs contained higher micronutrient elements concentrations than BCHs and APHs, e.g., Cu, Zn, Sr, Ge and Se (Table 5). Therefore, high REEs and micronutrient elements concentrations of hornblende-gneiss favored the synthesis and accumulation of flavonoid compounds in Scutellaria baicalensis after the activation of endocytosis induced by REEs [100,113]. In addition, trivalent lanthanum (La(III)) is similar to Ca^{2+} in terms of properties and structures as mentioned above. Therefore, La(III) may substitute for Ca^{2+} and present similar effects as Ca^{2+} in biological systems [105,114,115]. For instance, La(III) may bind to Ca-binding sites in the CaM molecule by electrostatic attraction or coordination [106,116] based on the concentrations of REEs. Hence, the CAM expression level in plants and its molecular structure was therefore affected by REE concentrations, affecting the accumulation of effective constituents [117].

Table 5. Parameters on micronutrient elements distribution characteristics of roots in various habitats, Hebei Province.

Micronutrient Elements	Habitats	Median (25∼75%) ($mg \cdot kg^{-1}$)	Average ($mg \cdot kg^{-1}$)	*p* Value
Cu	NGHs (n = 11)	11 (9.08–14.5)	12.2	0.277
	APHs (n = 10)	10.1 (7.59–11)	9.44	0.190
	BCHs (n = 8)	9.09 (6.85–11.8)	9.24	0.310
Zn	NGHs (n = 11)	15.9 (14.1–16.9)	15.3	0.806
	APHs (n = 10)	11.5 (10.53–13.2)	11.8	0.373
	BCHs (n = 8)	12.4 (11.58–17)	13.6	0.084
Sr	NGHs (n = 11)	48 (28.35–51.3)	48.3	0.039
	APHs (n = 10)	22.2 (20.8–25.7)	22.9	0.873
	BCHs (n = 8)	28.4 (22.26–34.7)	28.4	0.479
Ge	NGHs (n = 11)	1.21 (0.963–1.45)	1.28	0.004
	APHs (n = 10)	0.837 (0.777–0.995)	0.910	0.095
	BCHs (n = 8)	1.15 (0.829–1.57)	1.17	0.929
Se	NGHs (n = 11)	0.064 (0.045–0.069)	0.0592	0.818
	APHs (n = 10)	0.06 (0.045–0.063)	0.0550	0.686
	BCHs (n = 8)	0.045 (0.04–0.069)	0.0510	0.025

As mentioned above, we can conclude that parent materials significantly impact the quality of Scutellaria baicalensis in terms of micronutrient elements involving REEs. Some strategies for management of the habitats of *Scutellaria baicalensis* are as follows:

(1) Hornblende-gneiss locations were confirmed to be the natural top-geoherbs habitats of Rehe *Scutellaria baicalensis* for their relatively higher REEs and other micronutrient elements concentrations and soil property. In order to protect the chemical type of top-geoherbs, it was significant to avoid excessive digging of *Scutellaria baicalensis* to maintain their natural propagation and replacement.
(2) Luanping County and Kuancheng Kuancheng Manchu Nationality Autonomous County was also the main gneiss location in the Luanhe watershed in Chengde City. It can be considered for the large-scale cultivation of *Scutellaria baicalensis* by biomimetic cultivation.
(3) Scientific and reasonable rare earth micro-fertilizers application was optional for optimizing replanting patterns. The conventional principle that high micronutrient concentrations inhibit their absorption while low micronutrient concentrations favor their absorption should not be neglected.

6. Conclusions

This study presented the influences of parent materials on the inhabitation and quality of top-geoherb *Scutellaria baicalensis* in Chengde City, Hebei province, in terms of REEs. It was greatly significant for protecting the origin and optimizing replanting patterns of *Scutellaria baicalensis*. The migrations, enrichments, fractionations and transformations of REEs in the bedrock–regolith–soil–root continuum were studied in three habitats of *Scutellaria baicalensis* with contrasting geopedological conditions. Parent materials and soils in the hornblende-gneiss locations contained higher REE concentrations than loess locations. REE concentrations in loess soils were relatively homogeneous, while various mineral compositions and mineral grain sizes of the hornblende-gneiss resulted in the heterogeneity of REEs concentration in rhizosphere soils, with a coefficient of variation (CV) being 33.9% as weathering proceeded. Weathering, involving eluviation, leaching, absorption, etc., influenced the migrations and enrichments of REEs in weathering crust in hornblende-gneiss, and weathering productions, dominated by clay minerals and iron (hydro) oxide, controlled the fractionations within REEs. Roots of *Scutellaria baicalensis* contained similar ΣREE in NGHs (2.02 $mg{\cdot}kg^{-1}$) and BCHs (2.04 $mg{\cdot}kg^{-1}$), which are higher than that in APHs (1.78 $mg{\cdot}kg^{-1}$). It exhibited a remarkable positive correlation between REE concentrations in the roots and rhizosphere soils with a coefficient of 0.479 ($p < 0.01$). The biological absorption coefficients (BACs) of REEs for *Scutellaria baicalensis* decreased in the order of NGHs > APHs > BCHs. Soils developed in hornblende-gneiss were characterized by high REE concentrations, lower content of clay fraction and overall alkaline with a pH value of 8.06, favoring the inhabitation of Rehe *Scutellaria baicalensis* and adsorption for RREs. Micronutrient elements in the roots, e.g., REEs, Cu, Zn, Sr, Ge and Se, were remarkably correlated with flavonoid compound contents, suggesting their significant impact on the quality of *Scutellaria baicalensis*. The activation of endocytosis induced by REEs favored the adsorption of micronutrient elements and together improved the quality of *Scutellaria baicalensis*. Therefore, *Scutellaria baicalensis* in NGHs, featuring high REEs and other micronutrient elements concentrations, contained higher flavonoid compound content.

Author Contributions: Conceptualization, W.F. and Z.S.; methodology, Z.C. and Z.S.; software, T.A.; validation, L.X.; formal analysis, Z.S.; investigation, Z.C. and Z.S.; resources, H.Z.; data curation, L.X.; writing—original draft preparation, Z.S.; writing—review and editing, Z.S., W.F.; visualization, Z.S.; supervision, W.S. and H.Z.; project administration, Z.C. and H.Z. All authors have read and agreed to the published version of the manuscript.

Funding: This research was funded by the China Geological Survey Program (Grant No. DD20190822).

Institutional Review Board Statement: Not applicable.

Informed Consent Statement: Not applicable.

Data Availability Statement: Not applicable.

Acknowledgments: We would like to thank Wei Liu and Xiaoying Cui from Hebei Huakan Resource Environmental Survey Co., Ltd. for the test of REEs and flavonoid compounds.We thank Xia Li form China Institute of Geo-Environment Monitoring for financial support and Shoulin Zhang from Beijing Institute of Geology for Mineral Resources CO., LTD for valuable suggestions. We also thank editor and three anonymous reviewers for their valuable comments and suggestions

Conflicts of Interest: The authors declare no conflict of interest.

References

1. Hu, S. *Geoherbs in China*; Heilongjiang Science and Technology Press: Haerbin, China, 1989.
2. Xie, W. Discussion about geoherbs. *J. Tradit. Chin. Med.* **1990**, *40*, 43–46.
3. Huang, L.; Zhang, R. Biological essential about geoherbs. *Chin. Pharm. J.* **1997**, *32*, 563–566.
4. Huang, L.; Guo, L.; Ma, C.; Gao, W.; Yuan, Q. Top-geoherbs of traditional Chinese medicine: Common traits, quality characteristics and formation. *Front. Med.* **2011**, *5*, 185–194. [CrossRef] [PubMed]
5. Zhu, Y.G.; Duan, G.L.; Chen, B.D.; Peng, X.H.; Chen, Z.; Sun, G.X. Minerals Weathering and Elemental cycling in the System of Siols-microorganisms-plants. *Sci. Sin.* **2014**, *44*, 1107–1116.
6. Reimann, C.; Englmaier, P.; Fabian, K.; Gough, L.; Lamothe, P.; Smith, D. Biogeochemical plant–soil interaction: Variable element composition in leaves of four plant species collected along a south–north transect at the southern tip of Norway. *Sci. Total. Environ.* **2015**, *506*, 480–495. [CrossRef]
7. Yan, H.; Duan, J.A.; Qian, D.W.; Xiu, S.L.; Song, B.S.; He, Z.Q. Correlation Analysis and Evaluation of Inorganic Elements in Angelica sinensis and Its Correspondence Soil from Different Regions. *J. Chin. Med. Mater.* **2011**, *34*, 512–516.
8. Zhong, X.J.; Tan, Y.F. Research progress of soil factor influences on the quality of genuine medicinal materials. *J. South. Agric.* **2012**, *43*, 1708–1711.
9. Yao, Q.H.; Yan, S.A.; Zhang, B.L.; Su, H.G.; Pan, H.Y.; Lin, Q. Effects of Soil Types in Tea Garden on Distribution and Composition of Rare Earth Elements in Tieguanyin. *J. Trop. Subtrop. Bot.* **2018**, *26*, 644–650.
10. Tao, Y.; Shen, L.; Feng, C.; Qu, J.; Ju, H.; Yang, R.; Zhang, Y. Distribution of rare earth elements (REEs) and their roles in plants growth: A review. *Environ. Pollut.* **2022**, *298*, 118540. [CrossRef]
11. Qi, J.S.; Xu, H.B.; Zhou, J.Y.; Lu, X.H.; Yang, X.L.; Guan, J.H. Studies on the Amount of trace elements and Four Characteristics in Prescriptions of Chinese Medicine. *J. Anal. Sci.* **1998**, *14*, 283–287.
12. Zhang, Z.J.; Song, B. Effect Analyses on Micronutrient or REE Fertilization to Ginseng. *Liaoning Agric. Sci.* **1998**, *1*, 14–16.
13. Liu, C.E.; Ren, S.Y.; Yin, W.Y.; He, M.Y. Application Effect and Technique analyses of REE to the Eucommia ulmoides. *Hunan Agric. Sci.* **1999**, *27*, 29–31.
14. Chen, H.; Liu, H.L.; Dong, Y.Y. Study on the Relationship between Rare Earth Elements (REES)and Traditional Chinese Medicine(TCM). *Guangdong Trace Elem. Sci.* **2001**, *8*, 1–8.
15. Fu, W.; Li, X.; Feng, Y.; Feng, M.; Peng, Z.; Yu, H.; Lin, H. Chemical weathering of S-type granite and formation of rare earth element (REE)-rich regolith in South China: Critical control of lithology. *Chem. Geol.* **2019**, *520*, 33–51. [CrossRef]
16. Brantley, S.L.; Goldhaber, M.B.; Ragnarsdottir, K.V. Crossing disciplines and scales to understand the critical zone. *Elements* **2007**, *3*, 307–314. [CrossRef]
17. Hewawasam, T.; von Blanckenburg, F.; Bouchez, J.; Dixon, J.L.; Schuessler, J.A.; Maekeler, R. Slow advance of the weathering front during deep, supply-limited saprolite formation in the tropical Highlands of Sri Lanka. *Geochim. Cosmochim. Acta* **2013**, *118*, 202–230. [CrossRef]
18. Cheng, H.X.; Pei, M.; Zhao, C.D.; Hna, W.; Wang, H.Y.; Wang, Q.L.; Yang, F.; Zhang, F.G.; Wang, C.W.; Liu, F. Epigenetic geochemical dynamics and driving mechanisms of distribution patterns of chemical elements in soil, Southwest China. *Earth Sci. Front.* **2019**, *26*, 159–191.
19. Chinese Pharmacopoeia Commission. *The Pharmacopoeia of the People's Republic of China*; China Medical Science Press: Beijing, China, 2015.
20. Xie, Y.; Bi, J.H.; Peng, G.Y. Comparative Study on Detoxication between Dao-di Herb and Non Dao-di Herb of Huangqin. *Guid. J. Tradit. Chin. Med. Pharm.* **2015**, *21*, 35–38.
21. Liu, Y.; Li, L.T.; Ji, X.Q.; Kong, L.J.; Gao, Z.H.; Pang, J.; Chen, H.N.; Wang, S.M. Effect of inorganic element in soil on contents of inorganic elements and baicalin in *Scutellaria baicalensis* from different regions. *Chin. Tradit. Herb. Drugs* **2017**, *48*, 1225–1228.
22. Xin, X.J.; Li, Y.C.; Liu, G.J. Scutellaria Baicalensis Georgi Conformation Simulation Cultivation Technology In Daxing'An Mountains. *For. Sci. Technol. Inf.* **2016**, *48*, 20–21.
23. Liu, Y.Y.; Wu, P.P.; Yang, L.B.; Wang, L.M. Analysis of the Climate Characteridtics of thunderstorms in Chengde from 1973 to 2012. *Meteorol. J. Inn. Mong.* **2018**, *2*, 15–17.
24. Chen, D.; Chen, G. *Practical Geochemistry of Rare Earth Elements*; Geological Press: Beijing, China, 1990.
25. Yuan, M.; Guo, M.N.; Liu, W.S.; Liu, C.; van der Ent, A.; Morel, J.L.; Huot, H.; Zhao, W.Y.; Wei, X.G.; Qiu, R.L.; et al. The accumulation and fractionation of Rare Earth Elements in hydroponically grown Phytolacca americana L. *Plant Soil* **2017**, *421*, 67–82. [CrossRef]

26. Wang, J.; Wang, Z.H.; Geng, X.; He, F.P.; Zu, Y.C.; Wang, L. REE Biogeochemistry of Soil-Vegetation System in Dabaoshan Polymetallic Mine. *Earth Sci. J. China Univ. Geosci.* **2014**, *39*, 733–740.
27. Miao, L.; Xu, R.; Ma, Y.; Zhu, Z.; Wang, J.; Cai, R.; Chen, Y. Geochemistry and biogeochemistry of rare earth elements in a surface environment (soil and plant) in South China. *Environ. Geol.* **2008**, *56*, 225–235. [CrossRef]
28. Ryan, S.E.; Snoeck, C.; Crowley, Q.G.; Babechuk, M.G. 87Sr/86Sr and trace element mapping of geosphere-hydrosphere-biosphere interactions: A case study in Ireland. *Appl. Geochem.* **2018**, *92*, 209–224. [CrossRef]
29. Chen, D.; Zou, Z.; Ren, D. Preliminary application of plant exploration in search for Thallium mineral deposits. *Bull. Mineral. Petrol. Geochem.* **2000**, *19*, 397–400.
30. Hu, R.; Beguiristain, T.; De Junet, A.; Leyval, C. Bioavailability and transfer of elevated Sm concentration to alfalfa in spiked soils. *Environ. Sci. Pollut. Res.* **2020**, *27*, 44333–44341. [CrossRef]
31. Huang, L. *Molecular Pharmacognosy*; Peking University Medical Press: Beijing, China, 2006.
32. Xiao, Y.Q.; Jiang, Y.; Li, L.; Zhang, W.T.; Li, M.P.; Zhang, W.S. Relationship between active components in Scutellaria baicalensis and environmental factors in mountainous region of Western Beijing. *Chin. Tradit. Herb. Drugs* **2009**, *40*, 1291–1296.
33. Hu, Z.; Haneklaus, S.; Sparovek, G.; Schnug, E. Rare earth elements in soils. *Commun. Soil Sci. Plant Anal.* **2006**, *37*, 1381–1420. [CrossRef]
34. Loell, M.; Reiher, W.; Felix-Henningsen, P. Contents and bioavailability of rare earth elements in agricultural soils in Hesse (Germany). *J. Plant Nutr. Soil Sci.* **2011**, *174*, 644–654. [CrossRef]
35. Pye, K. Mineralogical and textural controls on the weathering of granitoid rocks. *Catena* **1986**, *13*, 47–57. [CrossRef]
36. Worthington, S.R.; Davies, G.J.; Alexander, E.C., Jr. Enhancement of bedrock permeability by weathering. *Earth-Sci. Rev.* **2016**, *160*, 188–202. [CrossRef]
37. Zhang, L.; Li, X.; Li, D.; Han, Z.; Zhang, G. Rare earth elements distribution and its correlation with microelements and particle-size of basalt-deriver soils in Leizhou Peninsula. *Acta Pedol. Sin.* **2011**, *48*, 1–9.
38. Brioschi, L.; Steinmann, M.; Lucot, E.; Pierret, M.C.; Stille, P.; Prunier, J.; Badot, P.M. Transfer of rare earth elements (REE) from natural soil to plant systems: Implications for the environmental availability of anthropogenic REE. *Plant Soil* **2013**, *366*, 143–163. [CrossRef]
39. Braun, J.J.; Riotte, J.; Battacharya, S.; Violette, A.; Prunier, J.; Bouvier, V.; Candaudap, F.; Maréchal, J.C.; Ruiz, L.; Panda, S.R.; et al. REY-Th-U solute dynamics in the critical zone: Combined influence of chemical weathering, atmospheric deposit leaching, and vegetation cycling (Mule Hole Watershed, South India). *Geochem. Geophys. Geosys.* **2017**, *18*, 4409–4425. [CrossRef]
40. Chang, C.; Song, C.; Beckford, H.O.; Wang, S.; Ji, H. Behaviors of REEs during pedogenetic processes in the karst areas of Southwest China. *J. Asian Earth Sci.* **2019**, *185*, 104023. [CrossRef]
41. Holdren, G.R., Jr.; Berner, R.A. Mechanism of feldspar weathering—I. Experimental studies. *Geochim. Cosmochim. Acta* **1979**, *43*, 1161–1171. [CrossRef]
42. Heckman, K.; Rasmussen, C. Lithologic controls on regolith weathering and mass flux in forested ecosystems of the southwestern USA. *Geoderma* **2011**, *164*, 99–111. [CrossRef]
43. Fu, S.Z.; Yan, C.L.; Wu, S.Q.; Yang, X.K. Content and Distribution Characteristics of Rare Earth Elements In Typical Soils Of Guizhou Province. *Acta Pedol. Sin.* **2000**, *37*, 109–115.
44. Miao, L.; Xu, R.S.; Xu, J.H. Geochemical Characteristics of Rare Earth Elements(REEs) in the Soil-Plant System in West Guangdong Province. *Acta Pedol. Sin.* **2007**, *44*, 54–62.
45. Mihajlovic, J.; Bauriegel, A.; St̕ark, H.J.; Roßkopf, N.; Zeitz, J.; Milbert, G.; Rinklebe, J. Rare earth elements in soil profiles of various ecosystems across Germany. *Appl. Geochem.* **2019**, *102*, 197–217. [CrossRef]
46. Coppin, F.; Berger, G.; Bauer, A.; Castet, S.; Loubet, M. Sorption of lanthanides on smectite and kaolinite. *Chem. Geol.* **2002**, *182*, 57–68. [CrossRef]
47. Tertre, E.; Berger, G.; Simoni, E.; Castet, S.; Giffaut, E.; Loubet, M.; Catalette, H. Europium retention onto clay minerals from 25 to 150 C: Experimental measurements, spectroscopic features and sorption modelling. *Geochim. Cosmochim. Acta* **2006**, *70*, 4563–4578. [CrossRef]
48. Galán, E.; Fernández-Caliani, J.; Miras, A.; Aparicio, P.; Márquez, M. Residence and fractionation of rare earth elements during kaolinization of alkaline peraluminous granites in NW Spain. *Clay Miner.* **2007**, *42*, 341–352. [CrossRef]
49. Borst, A.M.; Smith, M.P.; Finch, A.A.; Estrade, G.; Villanova-de Benavent, C.; Nason, P.; Marquis, E.; Horsburgh, N.J.; Goodenough, K.M.; Xu, C.; et al. Adsorption of rare earth elements in regolith-hosted clay deposits. *Nat. Commun.* **2020**, *11*, 4386. [CrossRef]
50. Andrade, G.R.P.; Cuadros, J.; Barbosa, J.M.P.; Vidal-Torrado, P. Clay minerals control rare earth elements (REE) fractionation in Brazilian mangrove soils. *Catena* **2022**, *209*, 105855. [CrossRef]
51. Land, M.; Òhlander, B.; Ingri, J.; Thunberg, J. Solid speciation and fractionation of rare earth elements in a spodosol profile from northern Sweden as revealed by sequential extraction. *Chem. Geol.* **1999**, *160*, 121–138. [CrossRef]
52. Laveuf, C.; Cornu, S. A review on the potentiality of rare earth elements to trace pedogenetic processes. *Geoderma* **2009**, *154*, 1–12. [CrossRef]
53. Steinmann, M.; Stille, P. Rare earth element behavior and Pb, Sr, Nd isotope systematics in a heavy metal contaminated soil. *Appl. Geochem.* **1997**, *12*, 607–623. [CrossRef]

54. Granados-Correa, F.; Vilchis-Granados, J.; Jiménez-Reyes, M.; Quiroz-Granados, L. Adsorption behaviour of La (III) and Eu (III) ions from aqueous solutions by hydroxyapatite: Kinetic, isotherm, and thermodynamic studies. *J. Chem.* **2013**, *2013*, 751696. [CrossRef]
55. Yusoff, Z.M.; Ngwenya, B.T.; Parsons, I. Mobility and fractionation of REEs during deep weathering of geochemically contrasting granites in a tropical setting, Malaysia. *Chem. Geol.* **2013**, *349*, 71–86. [CrossRef]
56. Yang, M.; Liang, X.; Ma, L.; Huang, J.; He, H.; Zhu, J. Adsorption of REEs on kaolinite and halloysite: A link to the REE distribution on clays in the weathering crust of granite. *Chem. Geol.* **2019**, *525*, 210–217. [CrossRef]
57. Jin, P.P.; Ou, C.H.; Ma, Z.G.; Li, D.; Ren, Y.J.; Zhao, Y.F. Evolution of montmorillonite and its related clay minerals and their effects on shale gas development. *Geophys. Prospect. Pet.* **2018**, *57*, 344–355.
58. Alshameri, A.; He, H.; Xin, C.; Zhu, J.; Wei, X.; Zhu, R.; Wang, H. Understanding the role of natural clay minerals as effective adsorbents and alternative source of rare earth elements: Adsorption operative parameters. *Hydrometallurgy* **2019**, *185*, 149–161. [CrossRef]
59. Zhang, Y.; Changan, L.; Xiong, D.; Zhou, Y.; Sun, X. Oxide geochemical characteristics and paleoclimate records of "Wushan loess". *Geol. China* **2013**, *40*, 352–360.
60. Cui, Y.; Luo, C.G.; Xu, L.; Zhang, H.; Deng, M.G.; Gu, H.N.; Meng, Y.; Qin, C.J.; Wen, H.J. Weathering Origin and Enrichment of Lithium in Clay Rocks of the Jiujialu Formation, Central Guizhou Province, Southwest China. *Bull. Mineral. Geochem.* **2018**, *37*, 696–704.
61. Quinn, K.A.; Byrne, R.H.; Schijf, J. Sorption of yttrium and rare earth elements by amorphous ferric hydroxide: Influence of pH and ionic strength. *Mar. Chem.* **2006**, *99*, 128–150. [CrossRef]
62. Huang, J.; Tan, W.; Liang, X.; He, H.; Ma, L.; Bao, Z.; Zhu, J. REE fractionation controlled by REE speciation during formation of the Renju regolith-hosted REE deposits in Guangdong Province, South China. *Ore Geol. Rev.* **2021**, *134*, 104172. [CrossRef]
63. Lee, Y.; Park, E.; Kim, W.; Choi, Y.; Park, J. A case of pelvic paragonimiasis combined with myoma uteri and pelvic inflammatory disease. *Korean J. Parasitol.* **1993**, *31*, 295–297. [CrossRef]
64. Takahashi, Y.; Minai, Y.; Ambe, S.; Makide, Y.; Ambe, F.; Tominaga, T. Simultaneous determination of stability constants of humate complexes with various metal ions using multitracer technique. *Sci. Total Environ.* **1997**, *198*, 61–71. [CrossRef]
65. Luo, Y.R.; Byrne, R.H. Carbonate complexation of yttrium and the rare earth elements in natural waters. *Geochim. Cosmochim. Acta* **2004**, *68*, 691–699. [CrossRef]
66. Sonke, J.E.; Salters, V.J. Lanthanide–humic substances complexation. I. Experimental evidence for a lanthanide contraction effect. *Geochim. Cosmochim. Acta* **2006**, *70*, 1495–1506. [CrossRef]
67. Zhao, Z.Z.; Xu, D.R.; Bi, H.; Tang, S.X. Vertical Distribution Pattern of REE Contents in Latosol in The Eastern Areas of Hainan Island. *Geotecton. Metallog.* **2006**, *30*, 401–407.
68. Pourret, O.; Davranche, M.; Gruau, G.; Dia, A. Competition between humic acid and carbonates for rare earth elements complexation. *J. Colloid Interface Sci.* **2007**, *305*, 25–31. [CrossRef]
69. Wan, Y.; Liu, C. The effect of humic acid on the adsorption of REEs on kaolin. *Colloids Surf. A Physicochem. Eng. Asp.* **2006**, *290*, 112–117. [CrossRef]
70. Li, Z. Study on Herbal Textual Research and Distribution and Change of Authentic Region of Huang Qin. Ph.D. Thesis, China Academy of Chinese Medical Sciences, Beijing, China, 2010.
71. Wyttenbach, A.; Furrer, V.; Schleppi, P.; Tobler, L. Rare earth elements in soil and in soil-grown plants. *Plant Soil* **1998**, *199*, 267–273. [CrossRef]
72. Ozaki, T.; Enomoto, S. Uptake of rare earth elements by Dryopteris erythrosora (autumn fern). *Riken Rev.* **2001**, *1*, 84–87.
73. Cao, X.; Ding, Z.; Hu, X.; Wang, X. Effects of soil pH value on the bioavailability and fractionation of rare earth elements in wheat seedling (Triticum aestivum L.). *Huanjing Kexue* **2002**, *23*, 97–102.
74. Tyler, G. Rare earth elements in soil and plant systems-A review. *Plant Soil* **2004**, *267*, 191–206. [CrossRef]
75. Semhi, K.; Chaudhuri, S.; Clauer, N. Fractionation of rare-earth elements in plants during experimental growth in varied clay substrates. *Appl. Geochem.* **2009**, *24*, 447–453. [CrossRef]
76. Gao, A.G.; Chen, Z.H.; Liu, Y.G.; Sun, H.Q.; Yang, S.Y. REE geochemical characteristics of surficial sediments in chukchi sea. *Sci. China Ser. D* **2003**, *33*, 148–154.
77. Jones, D. Trivalent metal (Cr, Y, Rh, La, Pr, Gd) sorption in two acid soils and its consequences for bioremediation. *Eur. J. Soil Sci.* **1997**, *48*, 697–702. [CrossRef]
78. Iyengar, S.; Martens, D.; Miller, W. Distribution and plant availability of soil zinc fractions. *Soil Sci. Soc. Am. J.* **1981**, *45*, 735–739. [CrossRef]
79. LeClaire, J.P.; Chang, A.; Levesque, C.; Sposito, G. Trace Metal Chemistry in Arid-Zone Field Soils Amended with Sewage Sludge: IV. Correlations between Zinc Uptake and Extracted Soil Zinc Fractions. *Soil Sci. Soc. Am. J.* **1984**, *48*, 509–513. [CrossRef]
80. Sims, J.T. Soil pH effects on the distribution and plant availability of manganese, copper, and zinc. *Soil Sci. Soc. Am. J.* **1986**, *50*, 367–373. [CrossRef]
81. Zhu, W.H.; Yang, Y.G.; Bi, H.; Liu, Q. Progress in Geochemical Research of Rare Earth Element in Soils. *Bull. Mineral. Petrol. Geochem.* **2003**, *23*, 259–264.
82. Ji, H.B.; Wang, L.J.; Dong, Y.S.; Wang, S.J.; Luo, J.M.; Sun, Y.Y. An Overview on the Study of Biogeochemical Cycle for Rare Earth Elements(REEs). *Prog. Geogr.* **2004**, *23*, 51–61.

83. Pang, X.; Xing, X.Y.; Wang, D.H.; Pei, A. Change of Rare-Earth Elements (REEs) Forms Using Them as Fertilizers. *Agro-Environ. Prot.* **2001**, *20*, 319–321.
84. Wang, X.; Liu, D. Integration of cerium chemical forms and subcellular distribution to understand cerium tolerance mechanism in the rice seedlings. *Environ. Sci. Pollut. Res.* **2017**, *24*, 16336–16343. [CrossRef]
85. Ding, S.; Liang, T.; Yan, J.; Zhang, Z.; Huang, Z.; Xie, Y. Fractionations of rare earth elements in plants and their conceptive model. *Sci. China Ser. C Life Sci.* **2007**, *50*, 47–55. [CrossRef]
86. Wang, L.F. Studies on the Photosynthetic Characterizations and Distributions of Rear Earth Elements in Fern Dicranopteris Dichotoma. Ph.D. Thesis, Institute of Botany, Chinese Academy of Sciences, Beijing, China, 2005.
87. Liang, M.X.; Chen, Z.B.; Chen, Z.Q.; Ren, T.J.; Qu, X. Effects of Vegetation Restoration on REEs Migration and Control in Red Soil Erosion Area in Southern China. *Chin. Rare Earths* **2022**, *43*, 64–72.
88. Shan, X.; Wang, H.; Zhang, S.; Zhou, H.; Zheng, Y.; Yu, H.; Wen, B. Accumulation and uptake of light rare earth elements in a hyperaccumulator Dicropteris dichotoma. *Plant Sci.* **2003**, *165*, 1343–1353. [CrossRef]
89. Chen, Z.; Chen, Z.; Bai, L. Rare earth element migration in gullies with different Dicranopteris dichotoma covers in the Huangnikeng gully group, Changting County, Southeast China. *Chemosphere* **2016**, *164*, 443–450. [CrossRef] [PubMed]
90. Khan, A.M.; Yusoff, I.; Abu Bakar, N.K.; Abu Bakar, A.F.; Alias, Y.; Mispan, M.S. Accumulation, Uptake and Bioavailability of Rare Earth Elements (Rees) in Soil Grown Plants from Ex-Mining Area in Perak, Malaysia. *Appl. Ecol. Environ. Res.* **2017**, *15*, 117–133. [CrossRef]
91. Yuan, Y.; Huang, H.L.; Liu, X.W. Influences of inorganic fertilizer on the effective constituent content. *Jiangxi For. Sci. Technol.* **2000**, *2*, 29–30.
92. Zhou, C.Z. Taxonomy and Systematic Research of Asarum Plants and Genuine Medicine. Ph.D. Thesis, Beijing University of Chinese Medicine, Beijing, China, 1994.
93. Lei, W.; Shui, X.; Zhou, Y.; Tang, S.; Sun, M. Effects of praseodymium on flavonoids production and its biochemical mechanism of Scutellaria viscidula hairy roots in vitro. *Pak. J. Bot.* **2011**, *43*, 2387–2390.
94. Zhou, J.; Fang, L.; Li, X.; Guo, L.; Huang, L. Jasmonic acid (JA) acts as a signal molecule in LaCl3-induced baicalin synthesis in Scutellaria baicalensis seedlings. *Biol. Trace Elem. Res.* **2012**, *148*, 392–395. [CrossRef]
95. Zhang, J.; Zhang, Y.; Jia, X.Y.; Sun, B.X.; Zhang, R.R.; Ma, C.G.; Liang, J.P. Nutrient uptake rules of *Polygala tenuifolia* and its relationship with accumulation of bioactive components. *J. Plant Nutr. Fertil.* **2019**, *25*, 1230–1238.
96. Fang, Y.M.; Cui, M.Y.; Liu, J.; Pei, T.L.; Wei, Y.K.; Zhao, Q. Study advance in biosynthesis of flavone from Scutellaria. *China J. Chin. Mater. Med.* **2020**, *43*, 4819–4826.
97. Guo, M.; Wu, Z.L.; Wang, C.G.; Gao, X.Y. Synthesis and anti-tumor activity of baicalin-metal complex. *Acta Pharm. Sin.* **2014**, *49*, 337–345.
98. Wang, Z.L.; Wang, S.; Kuang, Y.; Hu, Z.M.; Qiao, X.; Ye, M. A comprehensive review on phytochemistry, pharmacology, and flavonoid biosynthesis of *Scutellaria baicalensis*. *Pharm. Biol.* **2018**, *56*, 465–484. [CrossRef]
99. Sun, H.Y.; Sun, X.M.; Jia, F.C.; Wang, Y.L.; Li, D.J.; Li, J. The eco-geochemical characteristics of germanium and its relationship with the genuine medicinal material Scutellaria baicalensis in Chengde, Hebei Province. *Geol. China* **2020**, *47*, 1646–1667.
100. Bai, Y.C.; Wei, X.F.; Chen, L.; Wan, R.M.; Hou, Z.X. Multivariate Analysis of Fruit Leaf Mineral Elements, Soil Fertility Factors and Fruit Quality of Vaccinium uliginosum L. *Sci. Agric. Sin.* **2018**, *51*, 170–181.
101. Guo, B.S. Recent Research Advance of Rare Earth in the Field of Biology. *Chin. Rare Earths* **1999**, *20*, 64–68.
102. Hong, F.S.; Fang, N.H.; Gu, Y.H.; Zhao, G.W. Effect of Cerium Nitrate on Seed Vigor and Activitiesof Enzymes during Germination of Rice. *Chin. Rare Earths* **1999**, *20*, 45–47.
103. Jiang, L.; Zhang, W.C.; Wei, Z.L. Effects of micronutrient elements on cell growth and formation of flavonol glycosides of ginkgo callus. *Hubei Agric. Sci.* **1999**, *38*, 45–47.
104. Yuan, X.F.; Wang, Q.; Zhao, B.; Wang, Y.C. Promotion of Cell Growth and Flavonoids Production in Saussurea medusa Cell Suspension Cultures by Rare Earth Elements. *Chin. J. Process. Eng.* **2004**, *4*, 325–329.
105. Wang, J.N.; Huang, Y.H.; Mou, Z.M.; Wang, Y.W. Research Progress on Flavonoid of the Plant Secondary Metabolites. *Sci. Seric.* **2007**, *33*, 499–505.
106. Wang, L.; Cheng, M.; Chu, Y.; Li, X.; Chen, D.D.; Huang, X.; Zhou, Q. Responses of plant calmodulin to endocytosis induced by rare earth elements. *Chemosphere* **2016**, *154*, 408–415. [CrossRef]
107. Wang, L.; Li, J.; Zhou, Q.; Yang, G.; Ding, X.L.; Li, X.; Cai, C.X.; Zhang, Z.; Wei, H.Y.; Lu, T.H.; et al. Rare earth elements activate endocytosis in plant cells. *Proc. Natl. Acad. Sci. USA* **2014**, *111*, 12936–12941. [CrossRef]
108. Ben, Y.; Cheng, M.; Wang, L.; Zhou, Q.; Yang, Z.; Huang, X. Low-dose lanthanum activates endocytosis, aggravating accumulation of lanthanum or/and lead and disrupting homeostasis of essential elements in the leaf cells of four edible plants. *Ecotoxicol. Environ. Saf.* **2021**, *221*, 112429. [CrossRef] [PubMed]
109. Ge, Z.Q.; Li, J.C.; Yuan, Y.J.; Hu, Z.D. Effects of Ce (4+) on DNA Content and PAL Activity of Cell in Suspension Culture of Taxus Chinensis Var.Mairei. *Chin. Rare Earths* **2000**, *21*, 35–37.
110. Fang, Y.; Lv, W.M.; Hu, D.D.; Min, S.Z.; Cao, Z.Q. Interactions between baicalein and La(III), Nd(III), Sm(III), Yb(III) and Y(III). *J. Shaanxi Norm. Univ. (Nat. Sci. Ed.)* **1993**, *21*, 44–48.
111. Hu, Z.; Richter, H.; Sparovek, G.; Schnug, E. Physiological and biochemical effects of rare earth elements on plants and their agricultural significance: A review. *J. Plant Nutr.* **2004**, *27*, 183–220. [CrossRef]

112. Liu, Y.; Yang, Q.; Zhu, M.; Wang, L.; Zhou, Q.; Yang, Z.; Huang, X. Endocytosis in microcystis aeruginosa accelerates the synthesis of microcystins in the presence of lanthanum (III). *Harmful Algae* **2020**, *93*, 101791. [CrossRef]
113. Tang, L.; Lin, J.H.; Nian, G.X.; Li, Y.M.; Lin, Y.L.; Wang, S.; Liu, D.H. Effects of Cu, Zn and Se on contents of total flavonlid, chlorogenic acid and Se in the flower of Chrysanthemum morifolium Ramat. *Plant Nutr. Fertil. Sci.* **2009**, *15*, 1475–1480.
114. Yang, S.H.; Liu, X.F.; Guo, D.A.; Zheng, J.H. Effect of Rare-earth Element Eu (3+) on Callus Growth and Flavonoids Content in *Glycyrrhiza uralensis*. *J. Chin. Med. Mater.* **2005**, *28*, 533–534.
115. Ynag, S.H.; Liu, X.F.; Guo, D.A.; Zheng, J.H. Effects of Different Additives on Accumulation of Flavonoids in *Glycyrrhiza uralensis* Callus. *Chin. Pharm. J.* **2006**, *41*, 96–99.
116. Wang, L.; Lu, A.; Lu, T.; Ding, X.; Huang, X. Interaction between lanthanum ion and horseradish peroxidase in vitro. *Biochimie* **2010**, *92*, 41–50. [CrossRef]
117. Batistič, O.; Kudla, J. Analysis of calcium signaling pathways in plants. *Biochim. Biophys. Acta (BBA) Gen. Subj.* **2012**, *1820*, 1283–1293. [CrossRef]